Space Shuttle Separate-Surface Control-System Study

Lawrence W. Brown and
Raymond C. Montgomery

NASA

Space Shuttle Separate-Surface Control-System Study

Lawrence W. Brown and
Raymond C. Montgomery

Langley Research Center
Hampton, Virginia

INTRODUCTION

During reentry the trim angle of attack of the Space Shuttle nominally starts at 40° and decreases to about 5° with decreasing Mach number. This wide range of trim angle of attack creates special design considerations for both longitudinal and lateral-directional control. In the high-speed, high-angle-of-attack regime, the airflow over the vertical stabilizer is masked by the main body of the vehicle. Consequently, the rudder and speed brake are relatively ineffective and the vehicle is statically unstable. For the current design of the Shuttle, directional control and stability were provided through the use of a reaction control system (RCS) jet for yaw control which is operational down to Mach 1. Use of the RCS has worked well to date but is not fully satisfactory because (1) the control mechanization is on-off and not proportional, as is aerodynamic control by a rudder; (2) the RCS jet fuel usage during the reentry is uncertain and creates an added supply problem; (3) the jets are designed to expand into the full vacuum of outer space and not into the atmosphere as they would if used for control during entry. Hence, as atmospheric entry progresses and the need for control power increases, the effectiveness of the RCS jets decreases.

Various proposals have been made to obtain proportional aerodynamic yawing control moment using winglets, vertical fins, and other surfaces that would impact the structural design of the vehicle. This paper presents and evaluates a control-system concept designed to produce proportional yaw control moment by using the current Shuttle configuration without use of the RCS. Hence, it does not impact the structural design of the vehicle. The concept is called The Separate-Surface Control Concept because aerodynamic yaw-moment control is achieved by separate deflections of the inboard and outboard elevons on the existing Space Shuttle. These elevon surfaces are currently deflected simultaneously by using the digital flight control-system software.

This paper discusses the separate-surface concept as a function of individual surface deflection angle on the wing trailing edge. Independent pitch and roll control are achieved in the conventional manner, collectively deflecting all the surfaces for pitch and opposite deflection of the left and right elevon surfaces for roll. Independent yaw control is achieved by using differential deflection of the inboard and outboard elevons. The effects of the trim (the biases of the inboard and outboard surfaces from zero condition) and the deflection ratio (the incremental deflection of the individual surfaces from the trim condition) are illustrated. The method used to determine the control effectiveness for each of the surfaces and the calculation of the aerodynamic force and moment coefficients for a given control-surface position are presented. Numerical examples are used to illustrate the use of the separate-surface concept for stability augmentation. This concept is then incorporated in a lateral-control-system design to obtain satisfactory lateral handling qualities.

SYMBOLS

All aerodynamic data and flight motions are referenced to the body axis system.

$\left.\begin{array}{l} A,B,F,G, \\ H_1,H_2,H_3,H_4 \end{array}\right\}$ aerodynamic and control matrices

A_ϕ transfer function coefficient

a_Y lateral acceleration, g units

b wing span, ft

C_N normal-force coefficient, $\dfrac{\text{Normal force}}{qS}$

C_Y side-force coefficient, $\dfrac{\text{Side force}}{qS}$

C_l rolling-moment coefficient, $\dfrac{\text{Rolling moment}}{qSb}$

C_n yawing-moment coefficient, $\dfrac{\text{Yawing moment}}{qSb}$

c_{BF} body-flap mean chord, ft

c_{root} root mean chord, ft

c_{tip} tip chord, ft

$\bar{c}$ wing mean aerodynamic chord, ft

FRL   flight reference line

F_N normal force

h altitude, ft

I_X,I_Z moment of inertia about X- and Z-axis, slug-ft^2

M   Mach number

M_X,M_Z aircraft rolling and yawing moments

p,r aircraft roll and yaw rate about X and Z body axis, respectively, deg/sec or rad/sec

q dynamic pressure, $1/2\ \rho V^2$

RCS   reaction control system

S   wing area, ft^2

s Laplace transform function

2

$s(y)$ — length of control surface as a function of y, ft

T_R — roll-mode time constant, sec

T_S — spiral-mode time constant, sec

t_2 — time to double amplitude

$\vec{u}, \vec{u}_c$ — control and input vector

V — aircraft speed, m/sec (ft/sec)

V_∞ — free-stream speed, m/sec (ft/sec)

$\vec{x}$ — vector for $[p \quad \phi \quad r \quad \beta]^T$

x_{OR}, z_{OR} — components along the X and Z body axes of the right outboard surface

y — coordinate normal to plane of symmetry

$\vec{y}$ — vector for $[p \quad \phi \quad r \quad a_Y]^T$

α — angle of attack, deg

β — angle of sideslip, deg

δ_{BF} — body-flap deflection, deg

δ_I — inboard deflection, positive when trailing edge down, deg

$\delta_I/\delta_{I,c}, \delta_O/\delta_{O,c}$ — control interconnect ratios

δ_{IL} — left inboard deflection, negative when trailing edge up, deg

δ_{IR} — right inboard deflection, negative when trailing edge up, deg

δ_O — outboard deflection, positive when trailing edge down, deg

δ_{OL} — left outboard deflection, positive when trailing edge down, deg

δ_{OR} — right outboard deflection, positive when trailing edge down, deg

δ_a — aileron deflection, $\dfrac{\delta_{e,L} - \delta_{e,R}}{2}$, deg

δ_c — command input (δ_O or δ_I)

δ_e — elevon deflection, $\delta_O + \delta_I$, deg

δ_r — rudder deflection, deg

$\delta_{tr,I}$ — wing inboard trim angle, deg

$\delta_{tr,O}$ wing outboard trim angle, deg

$\zeta_{RS,1}, \zeta_{RS,2}$ oscillation spiral-roll coupled-mode damping ratios

ζ_d Dutch roll damping ratio

ζ_ϕ damping ratio for ϕ/δ_a transfer function numerator constant

$\lambda \pm i\omega$ complex roots of the characteristic equations

θ angle of pitch, deg

ρ air density, slugs/ft^3

ϕ angle of roll, deg

ϕ/β magnitude of ϕ/β transform polynomial evaluated for Dutch roll mode

ϕ/δ_I inboard transfer function

ϕ/δ_O outboard transfer function

ϕ/δ_a roll transfer function

ω_d Dutch roll frequency

$\omega_{RS,1}, \omega_{RS,2}$ oscillation spiral-roll coupled-mode frequencies

ω_ϕ natural frequency for ϕ/δ_a transfer function numerator

$(\omega_\phi/\omega_d)^2$ roll-yaw coupling parameter

Subscripts:

c command input

I inboard

L left

O outboard

R right

Derivatives:

$$C_{l_p} = \frac{\partial C_l}{\partial \left(\frac{pb}{2V}\right)} \qquad C_{l_r} = \frac{\partial C_l}{\partial \left(\frac{rb}{2V}\right)} \qquad C_{l_\beta} = \frac{\partial C_l}{\partial \beta} \qquad C_{l_{\delta_a}} = \frac{\partial C_l}{\partial \delta_a}$$

$$C_{l_{\delta_r}} = \frac{\partial C_l}{\partial \delta_r} \qquad C_{l_{\delta_I}} = \frac{\partial C_l}{\partial \delta_I} \qquad C_{l_{\delta_O}} = \frac{\partial C_l}{\partial \delta_O} \qquad C_{n_p} = \frac{\partial C_n}{\partial \left(\frac{pb}{2V}\right)}$$

4

$$C_{n_r} = \frac{\partial C_n}{\partial \left(\frac{rb}{2V}\right)} \qquad C_{n_{\delta_r}} = \frac{\partial C_n}{\partial \delta_r} \qquad C_{n_\beta} = \frac{\partial C_n}{\partial \beta} \qquad C_{n_{\delta_a}} = \frac{\partial C_n}{\partial \delta_a}$$

$$C_{n_{\delta_I}} = \frac{\partial C_n}{\partial \delta_I} \qquad C_{n_{\delta_O}} = \frac{\partial C_n}{\partial \delta_O} \qquad C_{Y_\beta} = \frac{\partial C_Y}{\partial \beta} \qquad C_{Y_{\delta_r}} = \frac{\partial C_Y}{\partial \delta_r}$$

$$C_{Y_{\delta_a}} = \frac{\partial C_Y}{\partial \delta_a} \qquad C_{Y_{\delta_I}} = \frac{\partial C_Y}{\partial \delta_I} \qquad C_{Y_{\delta_O}} = \frac{\partial C_Y}{\partial \delta_O}$$

$$C_{n_{\beta_{dyn}}} = C_{n_\beta} \cos \alpha - \frac{I_Z}{I_X} C_{l_\beta} \sin \alpha$$

A dot over a symbol indicates differentiation with respect to time. The superscript T indicates transpose of the matrix.

SEPARATE-SURFACE CONCEPT

The separate-surface concept utilizes the separation of the inboard and outboard elevons to achieve yawing-moment control. It takes advantage of the nonlinear nature of the incremental aerodynamic forces as a function of individual surface deflection angle on the wing trailing edge. The planform geometry of the Space Shuttle showing the separate surfaces is shown in figure 1. Moment control about all three body axes is achieved by separate deflections of the five trailing-edge surfaces shown in the planform - the body flap, the two inboard elevons, and the two outboard elevons. Independent pitch and roll control is achieved in a conventional manner, collectively deflecting all the surfaces for pitch and opposite deflection of the left and right elevon surfaces for roll. It is assumed that pitch trim is achieved by using the body flaps. Independent yaw control moment is achieved using differential deflection of the inboard and outboard elevons. For this to be effective in producing yawing moment, the inboard and outboard surfaces must be trimmed at different positions. Consider the case where the outboard elevons are biased down so that small deflection from trim modulates both lift and drag. If the inboard elevons can be trimmed so that some small deflection from trim modulates only lift to cancel the outboard modulated lift, yawing moment can be obtained with no change in rolling or pitching moment. This general concept will now be quantified by using Newtonian flow theory.

The Newtonian theory required for the analysis of the separate-surface concept is documented in reference 1. Basic assumptions underlying the theory are

1. The Mach number of the free stream is very large

2. On surfaces exposed to the flow, the component of momentum normal to the surface is lost, whereas the one parallel to the surface is unchanged

3. Shock waves are parallel to the free stream

4. A perfect vacuum exists in the wake of any object placed in the flow

Under these assumptions, the resultant force on a flat plate will be normal to the plate and pass through the area centroid of the plate. Thus, the incremental force acting on the right outboard elevon in figure 2 is given by

$$
\left.
\begin{aligned}
F_N &= \frac{1}{2} \rho V_\infty^2 S C_N = q S C_N \\[2ex]
C_N &= 2 \times \sin^2(\alpha + \delta)
\end{aligned}
\right\} \tag{1}
$$

and for the differential span element on the outboard elevon of the Space Shuttle (fig. 3), the incremental body axis forces and moments caused by the deflected outboard elevon are

$$
\left.
\begin{aligned}
dF_{N,OR} &= 2q \sin^2(\alpha + \delta_{OR}) \, s(y) \, dy \\[2ex]
dx_{OR} &= \sin(\delta_{OR}) \, dF_{N,OR} \\[2ex]
dz_{OR} &= -\cos(\delta_{OR}) \, dF_{N,OR} \\[2ex]
dM_{Z,OR} &= -y \, dx_{OR} \\[2ex]
dM_{X,OR} &= y \, dz_{OR}
\end{aligned}
\right\} \tag{2}
$$

The latter two equations can be integrated from the elevon split line to the tip of the elevon to get the total incremental forces and moments.

Equations (2) have been numerically integrated by using the Shuttle planform to produce the results presented in figure 4 (a graph of the incremental rolling and yawing moments as a function of surface deflection angle δ for the right inboard and outboard elevon surfaces). The data in figure 4 are plotted for an angle of attack of 25° and normalized to a common wing reference area of 3938 ft^2. As the angle of deflection of the control surface increases from -25°, the incremental moments vary from 0 (with a slope of 0). Of course, if the deflection is less than -25°, the surface will be in the wake of the wing and will produce no incremental moment. One significant point is that the inboard and outboard data points are almost coincident because of the current elevon geometry. In the range of deflections from -25° to 0°, the X body axis force component of the resultant acting on the control surface is negative, creating a slightly negative yawing moment. It is 0 at 0° deflection and then positive as the deflection is further increased. Thus, the yawing-moment curve crosses the zero abscissa of the graph at a deflection of 0°. Since the aerodynamic forces are proportional to the square of the sine of the sum of the angle of attack and the deflection angle of the surface, a nearly flat yaw-moment curve is produced for positive surface deflections.

6

The separate-surface concept takes advantage of the nonlinear nature of the incremental aerodynamic forces as a function of surface deflection angle on the wing trailing-edge surfaces. By biasing the outboard surfaces down to say 10°, an incremental change in outboard deflection will produce increments in both rolling and yawing moments. If the inboard surfaces are biased up to say -10°, an incremental deflection of those surfaces produces essentially only rolling moment. Thus, one technique for creating only yawing moment is to trim the vehicle with the biases discussed, to increment the outboard elevon to create both yawing moment and an added undesirable rolling moment, and to use the inboard elevon on the same side to cancel the undesirable rolling moment. The amount of yawing moment that can be achieved will depend on the trim setting of the inboard and outboard surfaces and on the incremental deflections of the individual surfaces from the trim condition. As an example, consider a trim setting of 0° for the inboard surfaces and +10° for the outboard surfaces. If the outboard surface on the right wing is deflected 10° down away from trim (total deflection of 20°), the resulting incremental coefficients will be -0.135 in yaw and +0.185 in roll (reading directly from fig. 4). Using the right inboard surface to balance the rolling moment (again from fig. 4), the required inboard deflection is -17°, which produces incremental coefficients of -0.01 in yaw and -0.185 in roll. Thus, the net accumulated coefficients are -0.125 in yaw and 0 in roll. These accumulated coefficients produce a yawing moment of 50 000 ft-lb at an altitude of 165 000 ft and $M = 10$. The most aft RCS jet produces 34 676 ft-lb with the center of gravity at 65 percent of body length and 32 275 ft-lb at 67 percent of body length. Because of this potential of achieving independent yawing control moment, the separate-surface concept is subsequently used herein to augment the directional stability of the Space Shuttle.

Separate-Surface Control Effectiveness

To evaluate the separate-surface concept for reentry, control effectiveness data are needed for each inboard and outboard surface. These data are not available from the existing Space Shuttle data base which assumed that the inboard and outboard surfaces move together and are not separated. Wind-tunnel tests have been made by assuming small separations of the inboard and outboard elevons in order to determine the effect of misalignment of the surfaces. The separation between the surfaces was less than 5°. Analysis presented in the last section by using Newtonian flow shows that the inboard and outboard surfaces have almost equal effectiveness in producing yawing and rolling moments. (See fig. 4.) This equal effectiveness provides a basis for extracting separate-surface data from the existing Space Shuttle data base. That is, if one assumes that the surfaces have equal effectiveness in producing roll and yaw moments, one may extract the moment coefficients from the Shuttle data base for, say, a combined left inboard and outboard deflection and halve them to get the moment coefficients for the individual inboard and outboard surfaces. Note that in the high-speed regime, this assumption is justified but its validity has not been established in the low-speed or supersonic regime.

A Space Shuttle data base digital computer program available at the Langley Research Center was used to generate the separate-surface control data base. The program calculates the aerodynamic force and moment coefficients for given control-surface positions from the data base. The aerodynamic derivatives used were taken from a 1975 data base (updated in ref. 2) and are presented for the trajectory of table 1 in table 2. To obtain these data from the data base program, the inboard and outboard surfaces are assumed to have equal effectiveness in producing rolling and yawing moments. The procedure for obtaining the control effectiveness data was to fix the elevon surface on one side at 0° and sweep the full-span elevon on the other

side through its range of surface deflections. The aerodynamic coefficients were obtained and the results were adjusted for the surfaces; for example, the roll and yaw coefficients were divided in half (fig. 5(a)). The usual sign convention used (that is, trailing edge down), which produces lift, was considered positive. Note that the general nonlinear feature of the yawing-moment data from Newtonian flow (fig. 4) is preserved for all flight conditions considered (fig. 5(b)). It is this nonlinear feature, namely the flat slope at negative deflections, that enables the separate-surface concept to be effective in producing yaw control. The aerodynamic coefficients for the surface deflections were tabulated so that the derivatives could be obtained for selected trim conditions. The inboard and outboard derivatives for two assumed trim conditions are presented in table 3. Also, for information, the side-force coefficients are shown in figure 5(c).

Flight Characteristics

The linearized body axis equations of motion were used to compute the flying quality parameters of table 4 and figures 6 and 7. Figure 6 shows that the basic Shuttle orbiter with fixed controls has a spiral-roll coupled mode and a Dutch roll mode with low frequency and damping. The negative roll-yaw coupling parameters $(\omega_\phi/\omega_d)^2$ shown in table 4 are indicative of roll reversal problems in which a positive aileron input would result in the vehicle starting to roll right and then roll left. The inability to achieve near pole-zero cancellation of the Dutch roll modes by conventional means is quite evident as shown in figure 7. The conventional means to correct undesirable roll-yaw coupling is to incorporate an aileron-to-rudder interconnect which serves to reduce the effective adverse yawing components and/or to rely on a yaw damper to provide sufficient Dutch roll damping so that no stability problems occur. For the current orbiter, this problem was solved by using an active control system which includes the reaction control system thrusters for yaw control.

In the absence of conventional means and to eliminate the dependency on the RCS, the inboard and outboard surface-control concept was considered as an added control for directional stability augmentation to obtain near pole-zero cancellation of the Dutch roll modes. With the proposed scheme, control is accomplished by trimming the inboard and outboard surfaces and coordinating the incremental deflections of all trailing-edge surfaces to effect moment control. With the surfaces trimmed, the ratio of the deflection of the inboard and outboard surfaces (which coordinate the deflections) determines the placement of the roll transfer function zeros. For the conventional control, the roll transfer function is

$$\frac{\phi}{\delta_a} = \frac{A_\phi\left(s^2 + 2\zeta_\phi\omega_\phi s + \omega_\phi^2\right)}{(s + 1/T_S)(s + 1/T_R)\left(s^2 + 2\zeta_d\omega_d s + \omega_d^2\right)} \tag{3}$$

With the separate-surface concept, the roll transfer function becomes

$$\frac{\phi}{\delta_c} = \frac{\phi}{\delta_0} + \frac{(\delta_I/\delta_0)\phi}{\delta_I} = \frac{A_{\phi,0}\left(s^2 + 2\zeta_{\phi,0}\omega_{\phi,0} s + \omega_{\phi,0}^2\right) + (\delta_I/\delta_0)\,A_{\phi,I}\left(s^2 + 2\zeta_{\phi,I}\omega_{\phi,I} s + \omega_{\phi,I}^2\right)}{(s + 1/T_S)(s + 1/T_R)\left(s^2 + 2\zeta_d\omega_d s + \omega_d^2\right)} \tag{4}$$

8

or

$$\frac{\phi}{\delta_c} = \frac{\left[A_{\phi,O} + (\delta_I/\delta_O)A_{\phi,I}\right]\left(s^2 + 2\zeta_{\phi,OI}\omega_{\phi,OI}s + \omega_{\phi,OI}^2\right)}{(s + 1/T_S)(s + 1/T_R)\left(s^2 + 2\zeta_d\omega_d s + \omega_d^2\right)} \tag{5}$$

The deflection ratio δ_I/δ_O of the inboard and outboard surfaces is the yaw control gain necessary to obtain near pole-zero cancellation of the Dutch roll modes.

The ϕ/δ_c transfer function zeros for an assumed trim condition, in which the inboard surfaces are up ($\delta_{tr,I} = -10°$) and the outboard surfaces are down ($\delta_{tr,O} = 10°$) with deflection ratios δ_I/δ_O of -1.9 and -2.8, were selected from early simulations and computations and are shown in figure 8. As shown, it would be quite difficult to obtain near pole-zero cancellation of the Dutch roll modes with a deflection ratio of -1.9 for conditions where $M > 2.99$. For a deflection ratio of -2.8, pole-zero cancellation can be obtained for the proposed Mach number range.

Control-System Design Criteria

The Space Shuttle orbiter is quite different in configuration and operational envelope than any other vehicle flown before. Consequently, large extrapolations had to be made to establish handling qualities for the atmospheric flight phase. For this study, the flying quality criteria were selected based, in part, on the study of references 3 and 4. From reference 3, the vehicle was considered to be of class III, category C, and have better than level 2 flying quality requirements. The parameters selected to evaluate and/or specify were the roll rate p time response, the roll time constant T_R, the spiral-mode time to double amplitude t_2, a limited sideslip β excursion, and the roll-yaw coupling parameter $(\omega_\phi/\omega_d)^2$.

Figure 9 shows the normalized roll rate p time response requirement boundaries for the flight control system in the hypersonic and the supersonic regime from reference 4. For a commanded roll rate ($p = 5$ deg/sec, ref. 3), the steady-state roll rate p should be reached in 10 sec. The roll-mode time constant given in reference 3 is consistent with this response and was selected as $T_R < 3.0$ sec. The spiral-mode time constant given in reference 3 is also considered satisfactory, and a minimum time to double amplitude of $t_2 > 12$ sec was selected.

The Dutch roll mode damping is considered satisfactory for a damping ratio of $\zeta_d > 0.02$ (ref. 3). The sideslip excursion is limited to $\beta < 2°$ in the current Shuttle because of dependence on the RCS system. In consideration of this limitation, a Dutch roll damping ratio was selected as being satisfactory for $\zeta_d > 0.15$. As indicated, the Space Shuttle orbiter exhibits roll reversal problems throughout the proposed trajectory. To insure that roll reversal is eliminated and to avoid sluggish response and pilot-induced oscillations, the roll-yaw coupling parameter was selected to be $0.8 < (\omega_\phi/\omega_d)^2 < 1.0$.

Open-Loop Step Control Responses

Linear system analysis was made for different assumed trim conditions and deflection ratios of the inboard and outboard surfaces. This analysis was to determine if turn coordination could be achieved by deflecting the wing trailing-edge surfaces alone by using the separate-surface concept. The roll rate p, the roll angle ϕ,

and the sideslip β responses for the open-loop unaltered configuration and selected cases for the altered (separate-surface) configuration are presented in figures 10 through 15 to show these conditions.

Figure 10 shows the responses for the open-loop unaltered configuration for a step aileron input δ_a of 2°. The responses (figs. 10(a) and (b)) show that roll reversal problems occur throughout the Mach number range (9.98 > M > 2.48). In addition, large induced sideslip angles are created (β > 3°) as shown in figure 10(c).

Figure 11 shows the response for an assumed trim condition in which the inboard surfaces are up ($\delta_{tr,I}$ = -10°) and the outboard surfaces are down ($\delta_{tr,O}$ = 10°), with a deflection ratio of the inboard to outboard surface of 0. For a step command outboard deflection of δ_O = 2° from trim, the right outboard surface is trailing edge down (δ_{OR} = 12°). The response shows a tendency for roll reversal. The roll rate starts negative but increases to p > 8 deg/sec for M < 4.47; hence, moderate roll angles develop, ϕ > 40° (figs. 11(a) and (b)). Favorable sideslip angles (sideslip angles in the opposite direction of the roll angles) are induced, β < -2.0° (fig. 11(c)).

Figure 12 shows the responses for an assumed trim condition where the inboard surfaces are level ($\delta_{tr,I}$ = 0°) and the outboard trailing-edge surfaces are down ($\delta_{tr,O}$ = 10°), with a deflection ratio which coordinates the deflections of the inboard to outboard surfaces of -1.9. For a step command input from trim of δ_c = 10°, the right inboard surface input is trailing edge up (δ_{IR} = -19°) and the right outboard surface input is trailing edge down (δ_{OR} = 10°). It should be recognized that these input deflections are for a linear system which is the same as a differential deflection of δ_{IR} = -9.5, δ_{IL} = 9.5, δ_{OR} = 5, and δ_{OL} = -5. The responses for M = 9.98 and M < 3.51 show roll reversal problems. The roll rate starts positive but becomes negative with small response amplitudes. In the Mach number range 4.47 > M > 3.98, there is very little response to the command input (figs. 12(a) and (b)). Adverse sideslips β (sideslips in the direction of the input) are exhibited for M = 9.98 and M < 3.51 (fig. 12(c)).

Figure 13 shows the responses for an assumed trim condition in which the inboard trailing-edge surfaces are up ($\delta_{tr,I}$ = -10°) and the outboard surfaces are down ($\delta_{tr,O}$ = 10°), with a deflection ratio of the inboard to outboard trailing-edge surfaces of -1.9. For a step command input from trim of δ_c = 10° (δ_O = 10°, δ_I = 10°), the right inboard surface input is trailing edge up (δ_{IR} = -19°) and the right outboard surface input is trailing edge down (δ_{OR} = 10°). The responses for M > 3.51 show a tendency for roll reversal; the roll rate starts negative but becomes increasingly large. In the range of M < 4.47, the roll rate becomes p > 20 deg/sec; hence, large roll angles develop (ϕ > 100°) (figs. 13(a) and (b)). In the Mach range 4.47 > M > 3.51, sideslip angles favorable to the input are induced β > -2.0°. In the lower Mach number range (M < 2.99), sideslip increases as Mach number decreases (β > -1.0°) (fig. 13(c)).

Figure 14 shows the responses for an assumed trim condition of $\delta_{tr,I}$ = -10° and $\delta_{tr,O}$ = 10°, with a deflection ratio of -2.8. For a step command input from trim of δ_c = 10° (δ_O = 10°, δ_I = 10°), the right inboard surface is up (δ_{IR} = -28°) and the right outboard surface is down (δ_{OR} = 10°). Roll reversal problems do not exist. For M = 9.98, the roll rate p is in the direction of the input but oscillates about the axis; hence, the roll angle ϕ remains about the axis. For the Mach range 4.47 > M > 2.99, the roll rate increases to p ≈ 15 deg/sec but decreases with Mach number. The roll angles are large (ϕ < 100°) and also decrease with Mach

number (figs. 14(a) and (b)). The sideslips β are adverse for $M = 9.98$ and $M < 3.51$ but are favorable in the range of $4.47 > M > 3.98$ (fig. 14(c)).

The rudder effectiveness for the separate-surface concept is of great interest in consideration of the proportional control feedback system. To indicate the contribution that could be obtained for the control system, responses for a rudder input are shown in figure 15. For an assumed trim condition of $\delta_{tr,I} = -10°$ and $\delta_{tr,O} = 10°$, with a rudder input of $\delta_r = -2°$, there are no responses for $M = 9.98$. This result is as expected because of the lack of rudder power (rudder derivatives are zero) at this Mach number. For the Mach number range of $M < 4.47$, the roll rate increases as Mach number decreases ($p > 10$ deg/sec); hence, the roll angle also increases ($\phi > 50°$) (figs. 15(a) and (b)). Small, favorable sideslips are induced, $\beta > -2°$ (fig. 15(c)). It should be noted that, as expected, a negative rudder deflection was necessary to obtain the desired responses.

It has been shown that the separate-surface concept can be used as a yaw control to obtain directional stability. For an assumed trim condition with a particular deflection ratio, the roll reversal problem was eliminated. It was also shown that the rudder is effective for $M < 4.47$, the effectiveness of which could be incorporated into a feedback control-system design.

LATERAL FLIGHT CONTROL-SYSTEM DESIGN

The inboard and outboard elevons and rudder surfaces were combined to obtain a control-system design that would provide satisfactory flying qualities. The basic linearized lateral equations of motion in body axes were in the form

$$\dot{\vec{x}} = A\vec{x} + B\vec{u} \tag{6}$$

where the state vector was represented as

$$\vec{x} = [p \quad \phi \quad r \quad \beta]^T \tag{7}$$

The control law was of the form

$$\vec{u} = G\vec{y} + F\vec{u}_c \tag{8}$$

where $\vec{u}$ and $\vec{u}_c$ are the inboard and outboard surface and rudder control and command input, respectively. To obtain the gains necessary to give satisfactory handling qualities, the control surfaces were considered to be deflected individually (δ_O, δ_I, and δ_r). The commanded deflections of the outboard ($\delta_{O,c}$) and the inboard ($\delta_{I,c}$) elevons were set equal to the control input where

$$\delta_c = 10° = \begin{Bmatrix} \delta_{O,c} = 10° \\ \delta_{I,c} = 10° \end{Bmatrix} \tag{9}$$

The interconnect ratios $\delta_I/\delta_{I,c}$ and $\delta_0/\delta_{0,c}$ which are fed forward by using the matrix where

$$F = \begin{bmatrix} \delta_0/\delta_{0,c} & 0 & 0 \\ 0 & \delta_I/\delta_{I,c} & 0 \\ 0 & 0 & 1 \end{bmatrix} \qquad (10)$$

Lateral acceleration feedback was used in the form

$$\vec{y} = H_1 \vec{x} + H_2 \vec{u} \qquad (11)$$

where the output vector was

$$y = [p \quad \phi \quad r \quad a_y]^T \qquad (12)$$

The closed-loop system takes the form

$$\dot{\vec{x}} = [A + B(I - GH_2)^{-1} GH_1]\vec{x} + [B(I - GH_2)^{-1}F]\vec{u}_c \qquad (13)$$

The implementation of the system as a two controller, a lateral and rudder control, would take the form

$$\dot{\vec{x}} = \begin{bmatrix} A + B(I - GH_2)^{-1} GH_1 \end{bmatrix}\vec{x} + \begin{bmatrix} BH_3 \mid BH_4 \end{bmatrix}\begin{bmatrix} \vec{u}_{c,1} \mid \vec{u}_{c,2} \end{bmatrix}^T \qquad (14)$$

where $\begin{bmatrix} BH_3 \mid BH_4 \end{bmatrix}$ and $\begin{bmatrix} \vec{u}_{c,1} \mid \vec{u}_{c,2} \end{bmatrix}^T$ are partitions of $\begin{bmatrix} B(I - GH_2)^{-1}F \end{bmatrix}$ and $\begin{bmatrix} \vec{u}_c \end{bmatrix}$.

The system represented by equation (13) was used in obtaining the feedback gains and the control interconnect ratios for satisfactory flying qualities.

A differential synthesis technique, explained in reference 5, was used to obtain the feedback gains and control interconnect ratios that produce selected flying quality parameters. In accordance with the previously discussed criterion, the spiral mode time constant T_S was selected to be the time to double amplitude of $t_2 = 12$ and the roll mode time constant as $T_R = 3.0$. The Dutch roll damping ratio was selected as $\zeta_d = 0.15$ with the frequencies close to the open-loop conditions and adjusted for the roll-yaw coupling parameter.

To eliminate the roll reversal problems, a deflection ratio of the inboard to outboard surfaces that would yield near pole-zero cancellation of the Dutch roll modes was selected. As shown in figure 8, it would be impossible to obtain near pole-zero cancellation of the Dutch roll mode with a deflection ratio δ_I/δ_0 of

-1.9 for $M > 2.99$. Therefore, a deflection ratio of -2.8 was selected and the roll-yaw coupling parameter was set to $(\omega_\phi/\omega_d)^2 = 1$. Feedback was assumed on the roll rate p, the yaw rate r, and the side-force acceleration a_Y. Also, with the inboard control interconnect ratio $\delta_I/\delta_{I,c}$ fixed, the outboard control interconnect ratio $\delta_O/\delta_{O,c}$ was allowed to vary to achieve the desired characteristics.

Table 5 shows the feedback gains and the control interconnect ratios that gave the flying quality parameters of table 6 for an assumed trim condition and deflection ratio of $\delta_I/\delta_O = 2.8$. Table 6 shows that the achieved characteristics are within the satisfactory handling quality specification with the exception of $M > 4.47$, and the feedback gains and interconnect ratios are small. For $M = 9.98$, the specification for the spiral mode $(1/T_s)$ and the roll-yaw coupling parameter $(\omega_\phi/\omega_d)^2$ were relaxed because of the aerodynamic restrictions.

Pole-zero cancellation was achieved throughout the Mach number range. In most cases, the Dutch roll damping ratios ζ_d were increased and the roll-yaw coupling parameters $(\omega_\phi/\omega_d)^2$ were decreased to reduce the sideslip β excursions. The responses for a step command input of $\delta_c = 10°$ from trim (fig. 16) show that for $M = 9.98$ the roll rate is small (p = 1.2 deg/sec); therefore, the roll angle is small with $\phi = 10°$ in 10 sec (figs. 16(a) and (b)). (The reader will note the change in the scales for this Mach number.) For $M < 4.47$, the responses show the system to be satisfactory. The roll rates meet the requirement of 5 deg/sec with a range of 18 deg/sec $>$ p $>$ 5 deg/sec, and it increases as Mach number decreases. The roll angles are also within the required $\phi = 30°$ with a range of 108° $>$ ϕ $>$ 37° and, as expected, increase as Mach number decreases. The sideslip angles are favorable in the Mach range $M < 4.47$ with $-2.4 < \beta < -1.4$ (fig. 16(c)), which also increases as the Mach number decreases.

Because of the sensitivity and the change in sign of some of the gains, a single set of feedback gains with an interconnect ratio that would give reasonable responses throughout the trajectory could not be obtained. However, for the trim condition and deflection ratio given, feedback gains and interconnect ratios that would give good handling qualities and show sensitivity from one condition to the next could be used in the range of $M < 4.47$. It should be recognized that at $M = 9.98$ the high angle of attack α and the low dynamic pressure q with an ineffective rudder caused higher than normal feedback gains.

Table 7 shows the feedback gains and the control interconnect ratios used to illustrate how the simple gains may be selected to indicate the sensitivity from one Mach number to the next. Table 8 shows that the flying quality parameters meet the accepted requirements except at $M = 3.98$ which shows a low Dutch roll damping ratio ζ_d. The responses for a step command input δ_c of 10° from trim (fig. 17) show that the roll rate responses are satisfactory (p = 5 deg/sec) with a range of 18.6 deg/sec $>$ p $>$ 5.7 deg/sec (fig. 17(a)). The roll angles are satisfactory (ϕ $>$ 30°) with a range of 100.5° $>$ ϕ $>$ 36° (fig. 17(b)). The sideslips are favorable in this range with $-2.68° < \beta < -1°$ (fig. 17(c)). The sideslip is large for $M = 2.99$ ($\beta = -20$); but, in consideration of the large roll angle ($\phi = 83.7°$), the sideslip would be within the required limit with a reduction in the commanded input.

CONCLUDING REMARKS

A separate-surface control-system concept has been presented for the Space Shuttle that allows for independent control of the moments about all three body axes by using the elevon and rudder as effectors. For this concept, control is

accomplished by trimming the inboard and outboard surfaces and coordinating the incremental deflection of all the trailing-edge surfaces to effect moment control. This trimming is necessary to eliminate roll reversal problems prevalent in the lateral responses. The concept was evaluated for hypersonic flight by using the Newtonian impact theory. Results indicate that at an altitude of 100 000 feet, where the rudder is masked by the body of the Shuttle, the effectiveness of the trailing-edge surfaces in producing yaw control moment is slightly greater than the most effective yaw jet. Further analysis was made with the Space Shuttle data base along with the STS-1 reentry trajectory with the assumption that the inboard and outboard surfaces had equal effectiveness. This assumption was justified in the hypersonic flow regime by Newtonian analysis. It has not been justified in the supersonic regime. A linearization of the lateral dynamics of the vehicle taken along the STS-1 reentry trajectory was used for flight control design and simulation studies. For an assumed trim condition and deflection ratio, near pole-zero cancellation of the Dutch roll mode was obtained and the vehicle exhibited substantial roll effectiveness. A control-system design with the inboard and outboard elevon and rudder surfaces as effectors was used to obtain satisfactory handling qualities. In the Mach number range $M < 4.47$, the specified satisfactory handling qualities were obtained. However, the absence of rudder effectiveness at high Mach numbers prevents obtaining satisfactory flying qualities. Flying qualities specifications were taken from the military specifications for class III piloted transport aircraft which may not be required at the hypersonic conditions in early entry.

These results imply that the concept can be used to eliminate the reaction control system (RCS) jet in the Space Shuttle orbiter for the $M < 4.47$ conditions and reduce the RCS jet for the higher Mach number conditions. It was also shown that, because of the large variation of system dynamics over the entire trajectory, there is a change in sign of some of the gains; therefore, a single set of feedback gains that would give reasonable response throughout the trajectory could not be obtained and, hence, gain scheduling is necessary.

Langley Research Center
National Aeronautics and Space Administration
Hampton, VA 23665
June 7, 1984

REFERENCES

1. Truitt, Robert Wesley: Hypersonic Aerodynamics. Ronald Press Co., c.1959, pp. 335-343.

2. Aerodynamic Design Data Book - Volume 1, Orbiter Vehicle STS-1. SD72-SH-0060 (Contract No. NAS9-14000), Rockwell International, 1980. (Available as NASA CR-160903.)

3. Military Specification - Flying Qualities of Piloted Airplanes. Mil-F-8785C, Nov. 5, 1980. (Supersedes Mil-F-8785B, Aug. 1969.)

4. Bayle, G. P.: Entry Flight Control Off-Nominal Design Considerations. AIAA Guidance and Control Conference - A Collection of Technical Papers, Aug. 1982, pp. 538-545. (Available as AIAA-82-1602.)

5. Montgomery, Raymond C.; and Hatch, Howard G., Jr.: The Application of a Differential Synthesis Technique to the Design of Multiaxis Stability Augmentation Systems for Aerospace Vehicles. AIAA Paper No. 68-834, Aug. 1968.

TABLE 1.- FLIGHT CONDITIONS

[Taken from the STS-1 trajectory]

Flight condition	Time, sec	h, ft	M	α, deg
1	1500	165 205	9.98	36.7
2	1743	107 213	4.47	19.1
3	1770	103 320	3.98	18.1
4	1795	98 150	3.51	17.7
5	1825	89 074	2.99	15.6
6	1855	79 813	2.48	13.0

TABLE 2.- SPACE SHUTTLE AERODYNAMIC CHARACTERISTICS

[Full-span elevon normal configuration]

Characteristic	Mach number of -					
	2.48	2.99	3.51	3.98	4.47	9.98
h, ft	81 921	91 181	100 257	105 428	109 321	165 205
V, fps	2429	2945	3481	3948	4473	10 801
q, psf	230.6	217.9	198.6	201.8	213.5	102.7
α, deg	12.97	15.64	17.73	18.08	19.07	36.74
θ, deg	6.87	5.26	7.44	9.25	11.23	19.66
C_{l_β}, rad^{-1}	-0.08508	-0.09736	-0.093127	-0.09235	-0.089023	-0.111698
C_{l_p}, rad^{-1}	-0.2358	-0.2331	-0.232388	-0.225389	-0.209421	-0.233191
C_{l_r}, rad^{-1}	0.08294	0.06157	0.053218	0.04442	0.04312	0.053368
C_{n_β}, rad^{-1}	-0.02535	-0.03715	-0.065272	-0.067418	-0.079509	-0.08225
C_{n_p}, rad^{-1}	0.57643	0.02947	0.012156	0.0036	-0.004869	-0.03467
C_{n_r}, rad^{-1}	-0.59423	-0.68425	-0.71733	-0.67615	-0.655605	-0.19698
C_{Y_β}, rad^{-1}	-0.814016	-0.75892	-0.66126	-0.606004	-0.54614	-0.384396
$C_{l_{\delta_a}}$, rad^{-1}	0.05783426	0.05148807	0.052662	0.05043524	0.050618	0.087528
$C_{l_{\delta_r}}$, rad^{-1}	0.01896856	0.01412199	0.01049847	0.00824998	0.0064387	0.00037291
$C_{n_{\delta_a}}$, rad^{-1}	-0.01817982	-0.01933198	-0.02051845	-0.0204856	-0.0197299	-0.0251199
$C_{n_{\delta_r}}$, rad^{-1}	-0.0345444	-0.02710487	-0.0204904	-0.0167461	-0.014335	0.0
$C_{Y_{\delta_a}}$, rad^{-1}	0.02037926	0.02240967	0.0187275	0.0137504	0.0150982	0.0221548
$C_{Y_{\delta_r}}$, rad^{-1}	0.06473893	0.04982006	0.0373516	0.0313866	0.026991	0.0

TABLE 3.- COMPUTED INBOARD AND OUTBOARD TRIM AERODYNAMIC CONTROL DERIVATIVES

Derivative	Mach number of -					
	2.48	2.99	3.51	3.98	4.47	9.98
$\delta_{tr,I} = 0°$; $\delta_{tr,O} = 10°$						
$C_{l_{\delta_{OR}}}$, rad^{-1} ...	-0.01827993	-0.01943307	-0.02249047	-0.02382299	-0.0235358	-0.02990048
$C_{l_{\delta_{IR}}}$, rad^{-1} ...	-0.01452954	-0.01309758	-0.0134137	-0.01287004	-0.01294023	-0.0223292
$C_{n_{\delta_{OR}}}$, rad^{-1} ...	0.01008192	0.01066759	0.01164571	0.01162981	0.01131873	0.01355067
$C_{n_{\delta_{IR}}}$, rad^{-1} ...	0.00480446	0.00507038	0.00538278	0.00537184	0.00518732	0.00657893
$C_{Y_{\delta_{OR}}}$, rad^{-1} ...	0.00165151	0.00355663	0.00204361	0.00010053	-0.00267496	-0.00722135
$C_{Y_{\delta_{IR}}}$, rad^{-1} ...	-0.00494631	-0.00539533	-0.00453503	-0.00336803	-0.00376499	-0.00559204
$\delta_{tr,I} = -10°$; $\delta_{tr,O} = 10°$						
$C_{l_{\delta_{OR}}}$, rad^{-1} ...	-0.01827993	-0.01943307	-0.02249047	-0.02382299	-0.0235358	-0.02990048
$C_{l_{\delta_{IR}}}$, rad^{-1} ...	-0.01217374	-0.01016829	-0.00955008	-0.00869736	-0.00832304	-0.0135731
$C_{n_{\delta_{OR}}}$, rad^{-1} ...	0.01008192	0.01066759	0.01164571	0.01162981	0.01131873	0.01344067
$C_{n_{\delta_{IR}}}$, rad^{-1} ...	0.000110348	0.00106438	0.00130659	0.00127594	0.00129593	0.00247557
$C_{Y_{\delta_{OR}}}$, rad^{-1} ...	0.00165151	0.00355663	0.00204361	0.00010053	-0.00267496	-0.00722135
$C_{Y_{\delta_{IR}}}$, rad^{-1} ...	-0.00333275	-0.00524694	-0.00451154	-0.00338075	-0.00316188	-0.00481593

TABLE 4.- LATERAL FLYING QUALITY PARAMETERS FOR UNAUGMENTED SPACE SHUTTLE

Parameter	Mach number of —					
	2.48	2.99	3.51	3.98	4.47	9.98
α, deg	12.97	15.64	17.73	18.08	19.07	36.74
$\lambda_1 \pm \omega_1$	-0.04473 ± 0.06101	-0.04396 ± 0.03855	-0.03375 ± 0.03539	-0.02898 ± 0.0301	-0.0255 ± 0.02789	-0.00314 ± 0.00283
$\lambda_2 \pm \omega_2$	-0.1141 ± 0.8925	-0.08237 ± 1.0313	-0.0635 ± 0.9661	-0.0544 ± 0.9775	-0.04767 ± 0.9868	-0.00958 ± 1.2152
Period 1	83.059	107.462	128.482	150.402	166.274	1487.5
Period 2	6.983	6.073	6.4896	6.4177	6.630	5.170
$\zeta_{RS,1}$	0.5912	0.7519	0.6902	0.6937	0.6746	0.7429
$\zeta_{RS,2}$	0.1268	0.0796	0.06559	0.05557	0.04826	0.00788
$\omega_{RS,1}$	0.07565	0.05847	0.0489	0.04178	0.03779	0.00422
$\omega_{RS,2}$	0.8998	1.0346	0.9682	0.9790	0.9879	1.2152
$(\omega_\phi/\omega_d)^2$	-0.5637	-0.5257	-0.7155	-0.7233	-0.8248	-0.2759
ϕ/β	6.140	5.021	5.077	5.027	5.094	2.0528
ζ_ϕ	-0.0728	-0.0557	-0.0392	-0.0321	-0.02637	-0.002433
ω_ϕ	-0.6755	-0.7501	-0.8190	-0.8326	-0.8972	-0.6383
$C_{n_{\beta_{dyn}}}$, rad^{-1}	0.1333	0.1836	0.1758	0.1767	0.1697	0.5930

TABLE 5.- FEEDBACK GAINS AND CONTROL INTERCONNECT RATIOS FOR
AUGMENTING SPACE SHUTTLE WITH INBOARD AND OUTBOARD
ELEVON AND RUDDER SURFACES

M	α, deg	G				F		
		p	ϕ	r	a_Y	δ_{OR}	δ_{IR}	δ_r
2.48	12.97	0.7349	0	0.06806	-1.151	1.880		
		0.8072	0	-0.4871	-0.5951		-2.8	
		0.4605	0	-1.9709	1.892			1.0
2.99	15.64	0.6397	0	0.2566	0.6255	1.0587		
		0.6605	0	0.1333	0.3399		-2.8	
		0.8896	0	-0.4708	-0.3783			1.0
3.51	17.73	0.8592	0	0.8867	0.2189	0.9717	0	0
		0.9240	0	0.3302	0.1371	0	-2.8	0
		1.7859	0	-0.6067	0.1063	0	0	1.0
3.98	18.08	0.9938	0	1.797	-1.477	0.9655	0	0
		1.047	0	0.3019	-0.4965	0	-2.8	0
		2.6084	0	-2.164	0.6951	0	0	1.0
4.47	19.07	0.8452	0	1.773	-0.7451	0.8889	0	0
		1.010	0	0.4378	-0.1729	0	-2.8	0
		2.982	0	-1.207	0.5680	0	0	1.0
9.98	36.74	-6.836	0	-2.1995	2.857	1.0782		
		17.936	0	5.335	1.817		-2.8	
		-0.8865	0	-0.2632	-0.0609			1.0

TABLE 6.- FLYING QUALITY PARAMETERS FOR AUGMENTED SPACE SHUTTLE

Parameter	Mach number of –					
	2.48	2.99	3.51	3.98	4.47	9.98
α, deg	12.97	15.64	17.73	18.08	19.07	36.74
$1/T_S$	0.05504	0.05613	0.05526	0.05395	0.05257	-0.00312
$1/T_R$	-0.3435	-0.3176	-0.3352	-0.3556	-0.3659	-0.3195
$\lambda \pm \omega i$	$-0.2600 \pm 1.3390i$	$-0.1178 \pm 0.5180i$	$-0.1454 \pm 0.6973i$	$-0.1798 \pm 1.0672i$	$-0.1468 \pm 0.9326i$	$-0.09314 \pm 0.4645i$
Period	4.6065	11.8266	8.8213	5.8059	6.6553	13.263
ζ_d	0.1906	0.2218	0.2042	0.1661	0.1555	0.1966
ω_d	1.3640	0.5313	0.7123	1.0822	0.9441	0.4737
$\left(\dfrac{\omega_{\phi,OI}}{\omega_d}\right)^2$	1.0147	0.8254	0.8752	0.9590	0.9016	0.6926
ϕ/β	4.1916	8.8258	5.8076	4.2555	4.5763	4.167
$\zeta_{\phi,OI}$	-0.1713	-0.1626	-0.2711	-0.3488	-0.3672	1.298
$\omega_{\phi,OI}$	1.3740	0.4827	0.6663	1.0598	0.8964	0.3943

TABLE 7.— FEEDBACK GAINS AND CONTROL INTERCONNECT RATIOS
USED FOR SENSITIVE EVALUATION

M	α, deg	G				F		
		p	ϕ	r	a_Y	δ_{OR}	δ_{IR}	δ_r
2.48	12.97	0.7	0	-0.2	-0.63	1.8	0	0
		0.7	0	-0.75	-0.05	0	-2.8	0
		0.4	0	-0.05	1.8	0	0	1.0
2.99	15.64	0.6	0	0.3	0.63	1.09	0	0
		0.6	0	0.15	0.35	0	-2.8	0
		0.83	0	-0.47	-0.36	0	0	1.0
3.51	17.73	0.8	0	0.9	0.23	0.99	0	0
		0.9	0	0.35	0.15	0	-2.8	0
		1.73	0	-0.57	0.14	0	0	1.0
3.98	18.08	0.9	0	1.1	-0.37	0.9	0	0
		0.9	0	0.05	0.05	0	-2.8	0
		2.5	0	-1.8	0.7	0	0	1.0
4.47	19.07	0.9	0	1.7	-0.67	0.9	0	0
		0.9	0	0.45	-0.15	0	-2.8	0
		2.9	0	-1.2	0.6	0	0	1.0
9.98	36.74	-7.52	0	-2.2	2.8	1.08	0	0
		19.6	0	5.8	1.8	0	-2.8	0
		-0.97	0	-0.27	-0.06	0	0	1.0

TABLE 8.- FLYING QUALITY PARAMETERS FOR SENSITIVE STUDY

Parameter	Mach number of –					
	2.48	2.99	3.51	3.98	4.47	9.98
α, deg	12.97	15.64	17.73	18.08	19.07	36.74
$1/T_S$	0.0422	0.0715	0.0502	0.0457	0.0622	0.00017
$1/T_R$	-0.3285	-0.2539	-0.3448	-0.3881	-0.2998	-0.2494
$\lambda \pm \omega i$	$-0.2699 \pm 1.2857i$	$-0.1427 \pm 0.5261i$	$-0.1156 \pm 0.7204i$	$-0.0712 \pm 0.9193i$	$-0.2016 \pm 0.9182i$	$-0.1331 \pm 0.4334i$
Period	4.783	11.526	8.612	6.814	6.683	13.858
ζ_d	0.2055	0.2618	0.1584	0.0772	0.2144	0.2994
ω_d	1.3137	0.5452	0.7296	0.9220	0.9401	0.4534
$\left(\dfrac{\omega_{\phi,OI}}{\omega_d}\right)^2$	1.053	1.156	1.029	0.895	1.037	0.848
ϕ/β	4.141	8.945	5.618	4.481	4.716	4.397
$\zeta_{\phi,OI}$	-0.1057	-0.1644	-0.2643	-0.3217	-0.3595	-0.3218
$\omega_{\phi,OI}$	1.3481	0.5860	0.7401	0.8725	-0.9573	0.4174

$c_{tip} = 60$ in.

$c_{root} = 119$ in.

$c_{BF} = 81$ in.
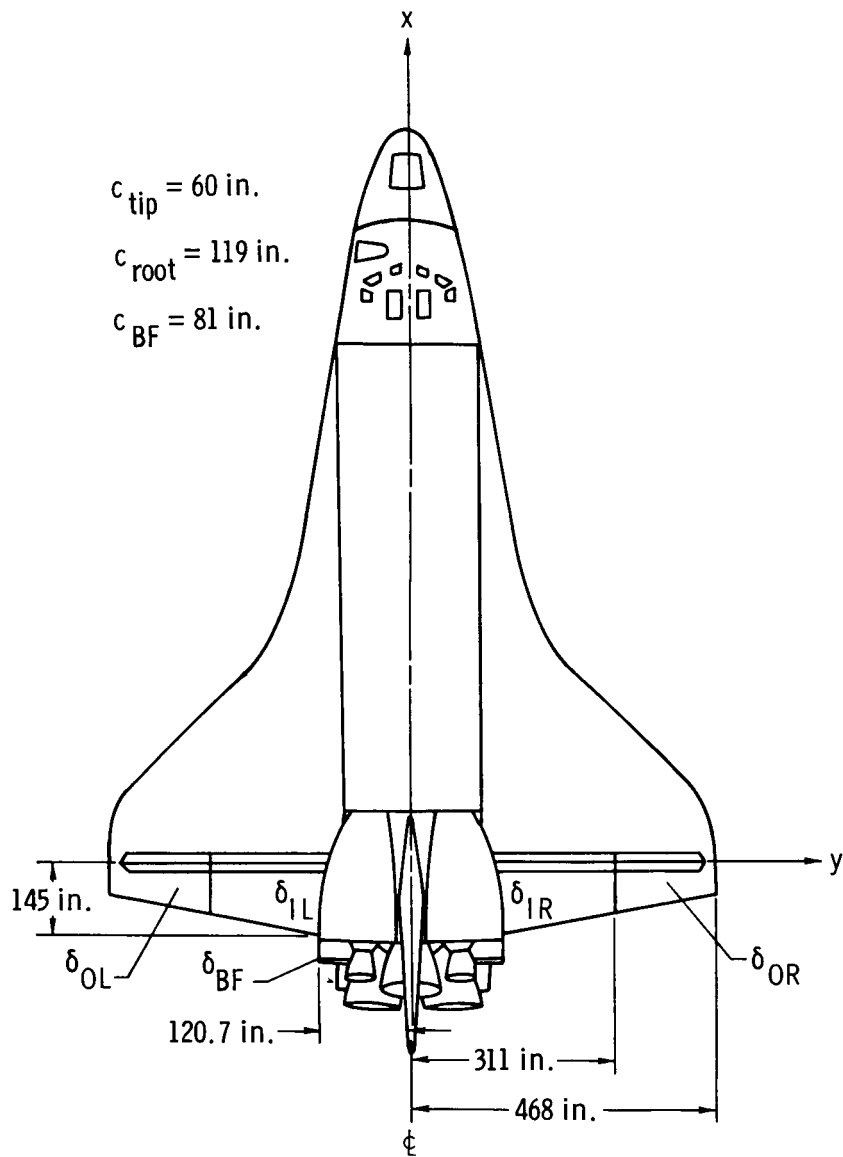
Figure 1.- Planform geometry of Space Shuttle
showing separate surfaces.
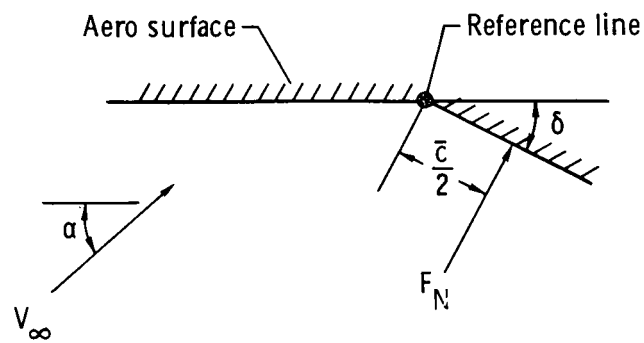
Figure 2.- Aerodynamic force representation
used for Newtonian flow.
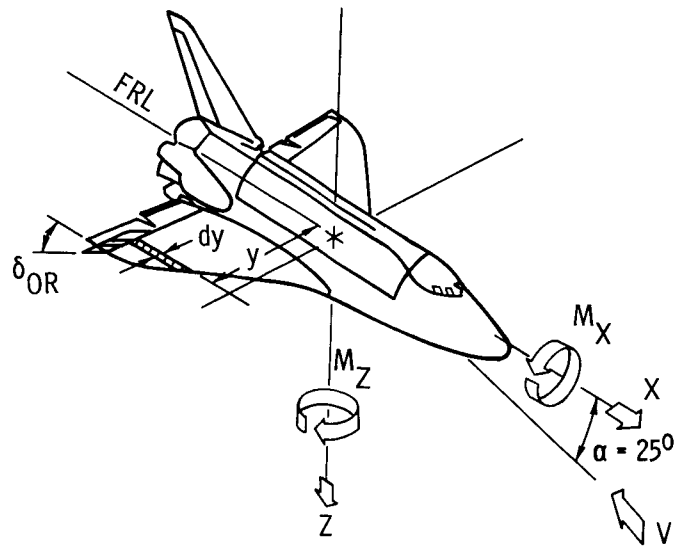
Figure 3.- Forces and moments for outboard
deflection for β = 0°.
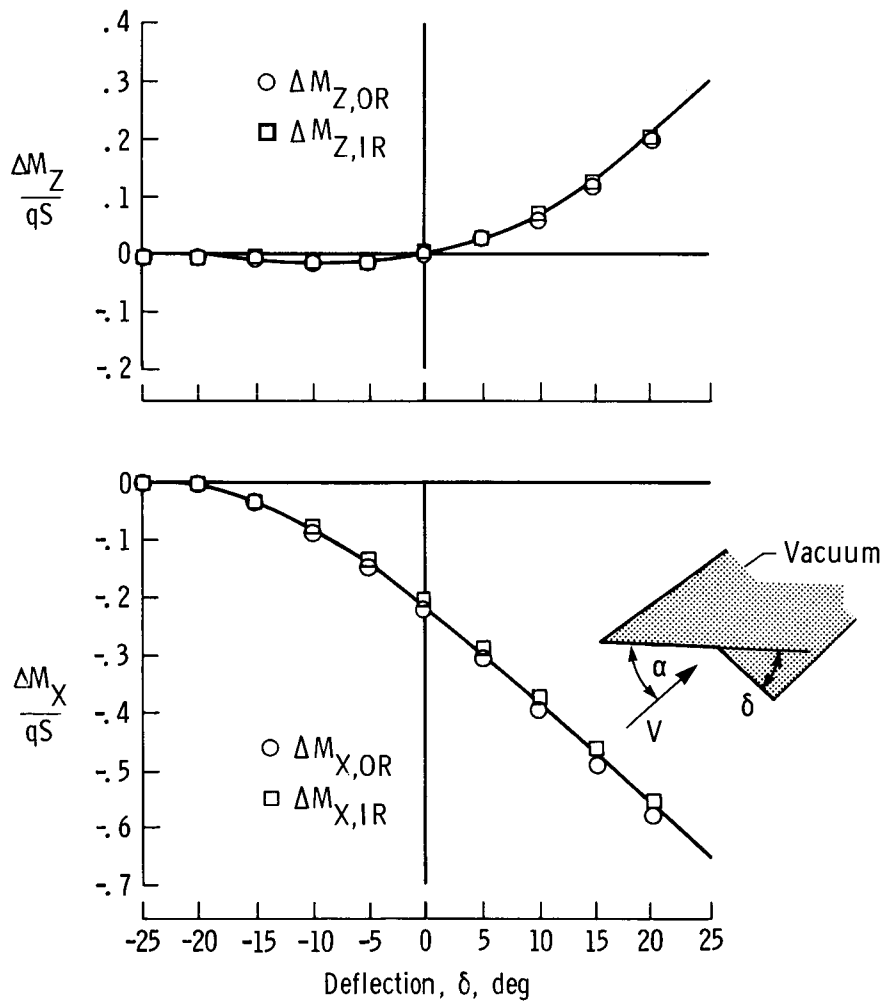
Figure 4.- Separate-surface control effectiveness.
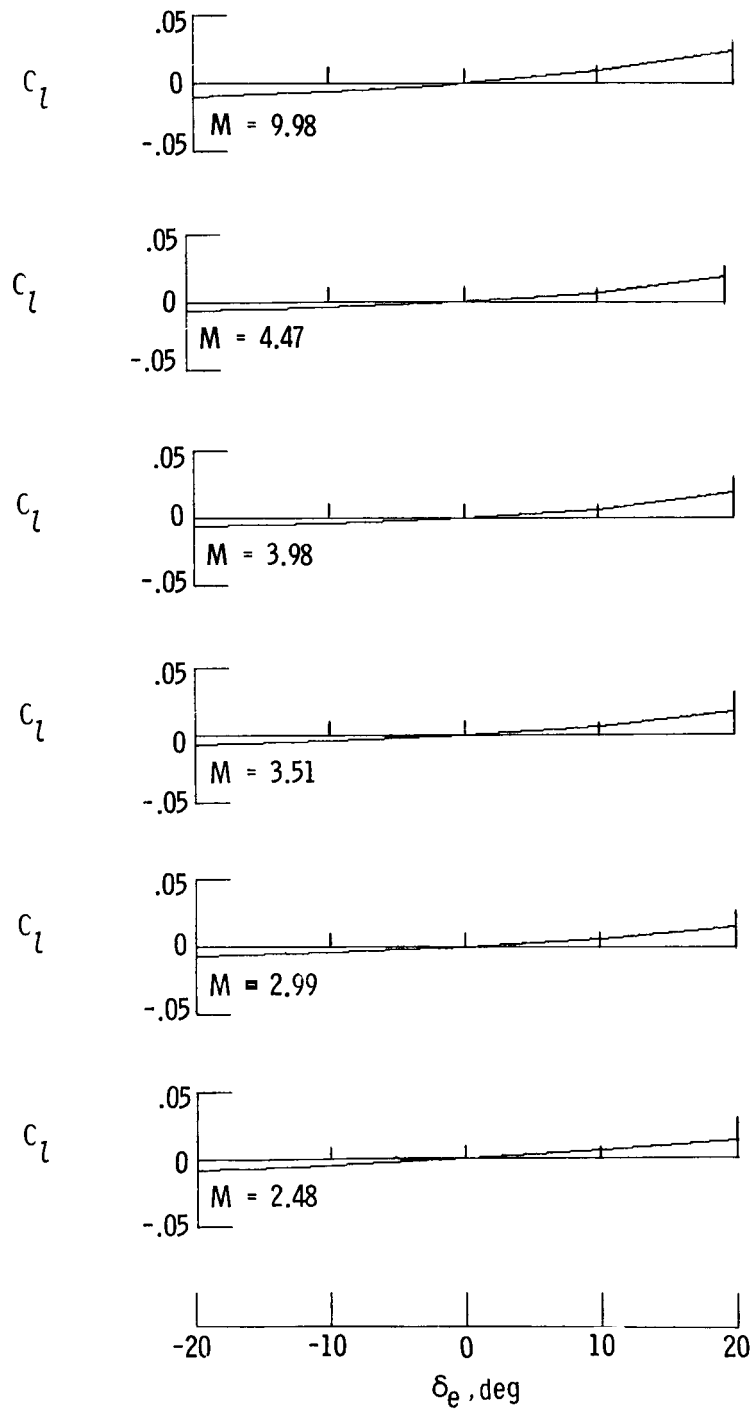
(a) Rolling moments.

Figure 5.- Lateral-control capability for separate surface.
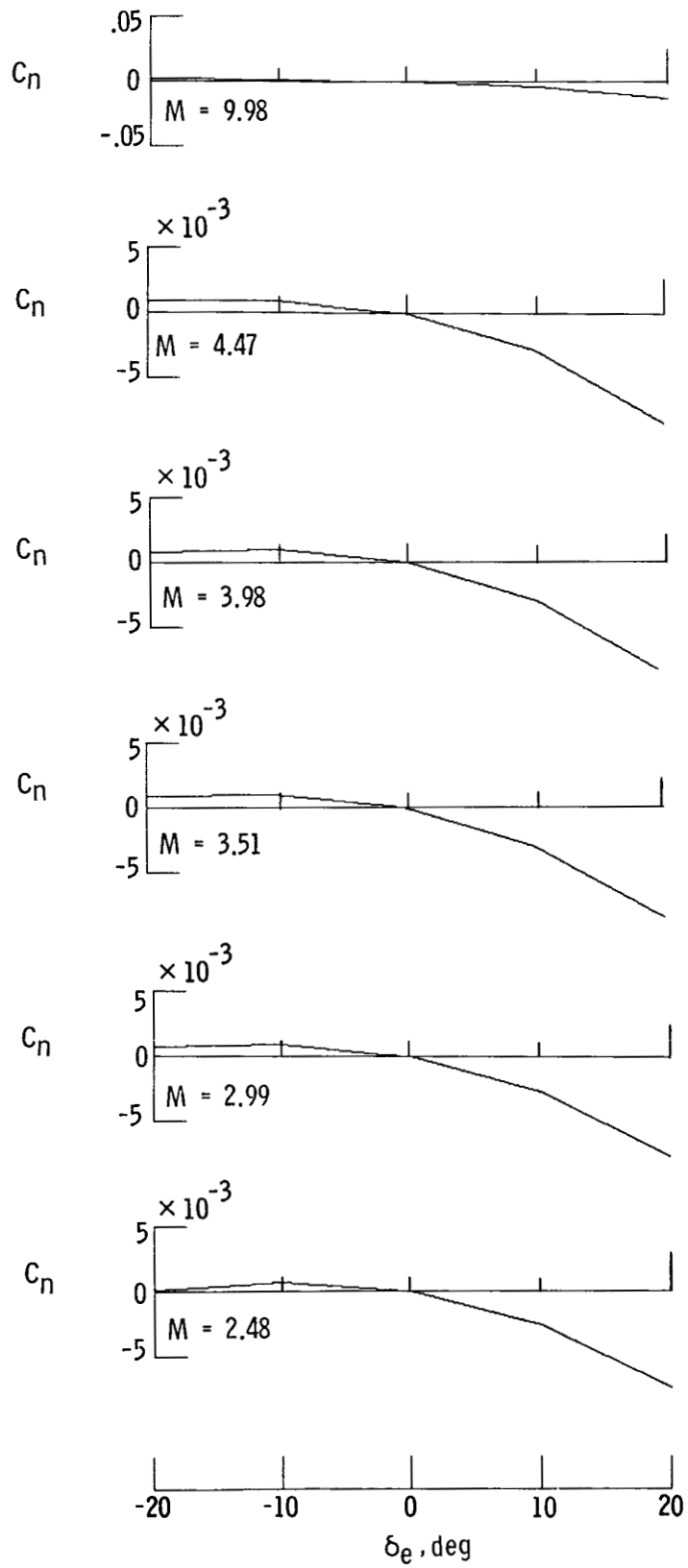
(b) Yawing moments.

Figure 5.- Continued.
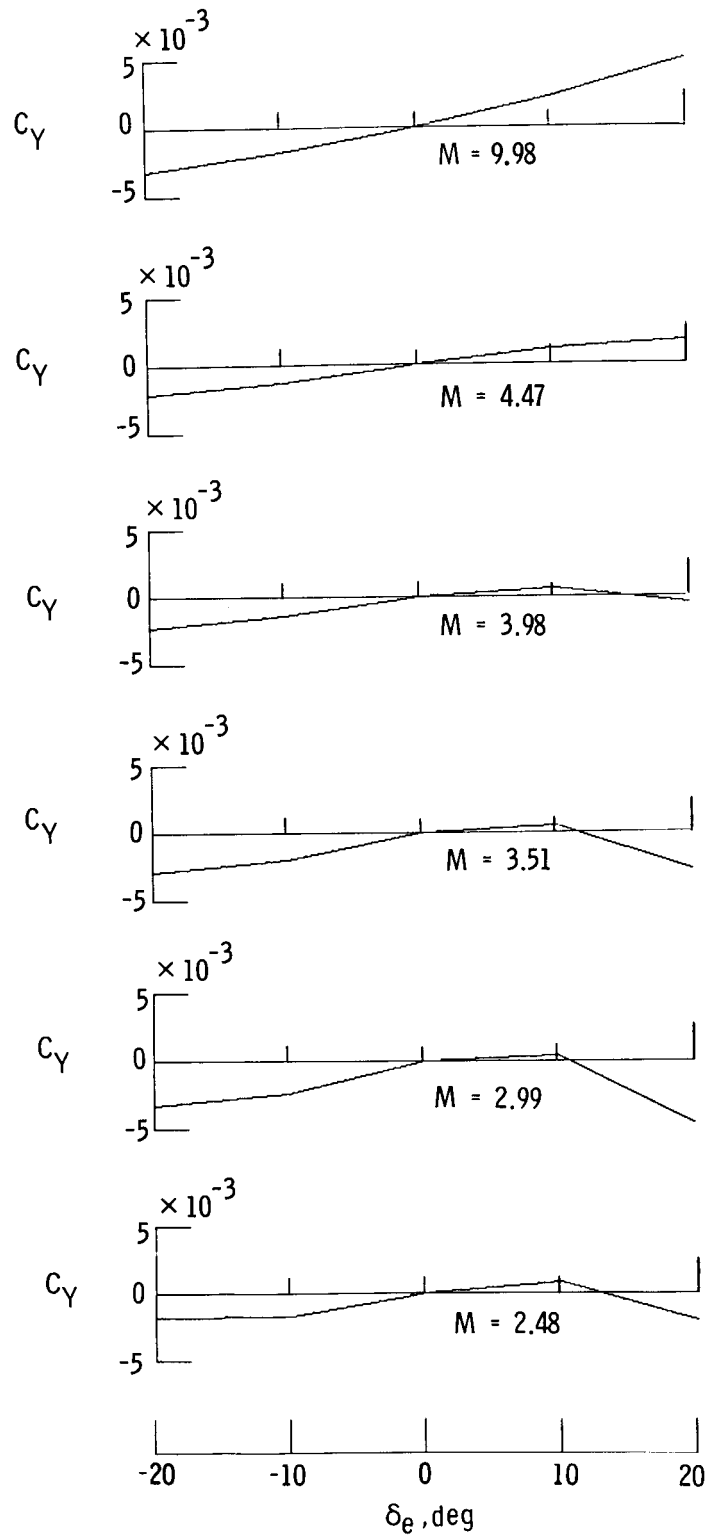
(c) Side force.

Figure 5.- Concluded.
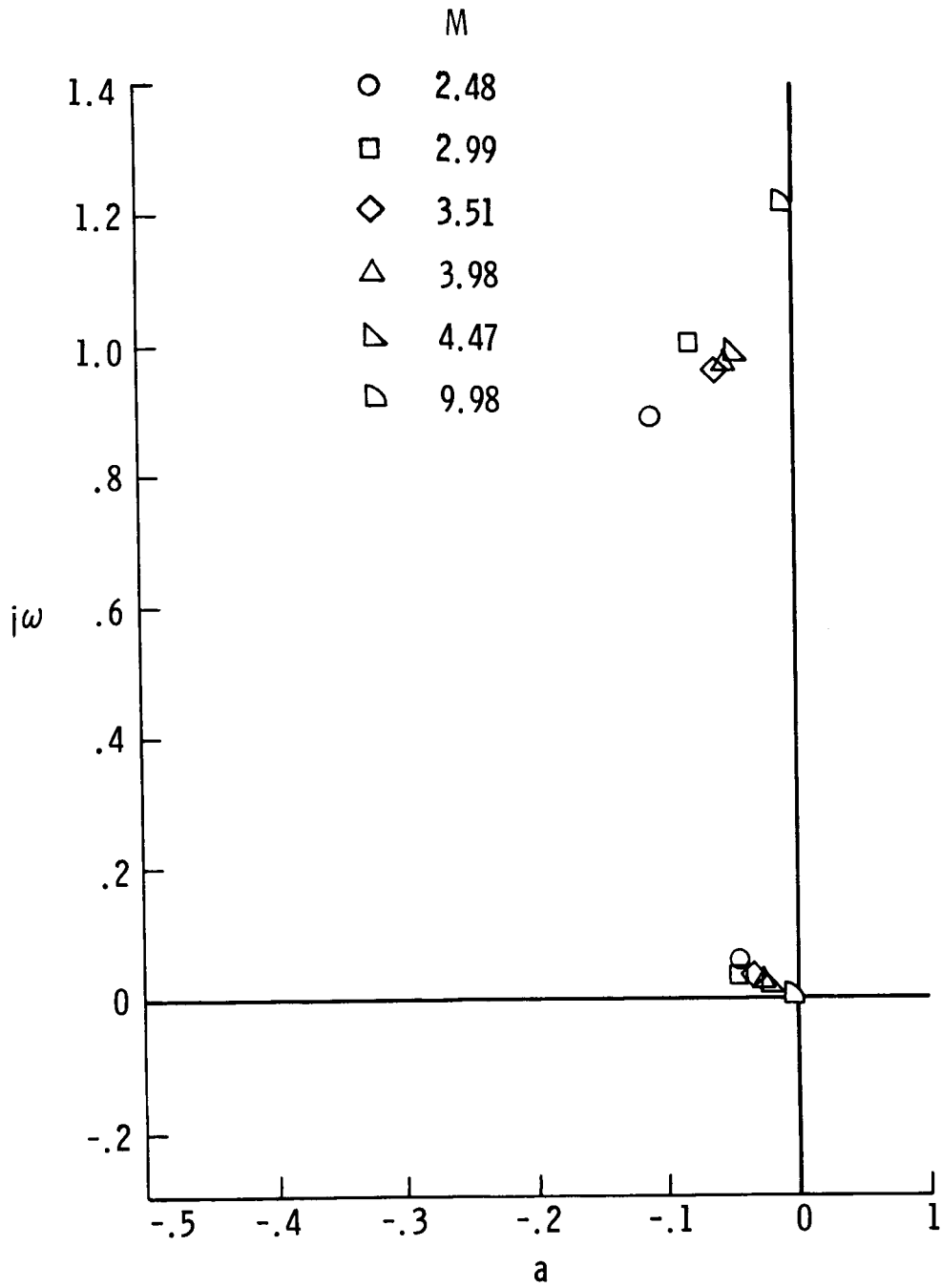
Figure 6.- Root locus poles for normal unaugmented Shuttle configuration.

M	
○	2.48
□	2.99
◇	3.51
△	3.98
◁	4.47
⬠	9.98
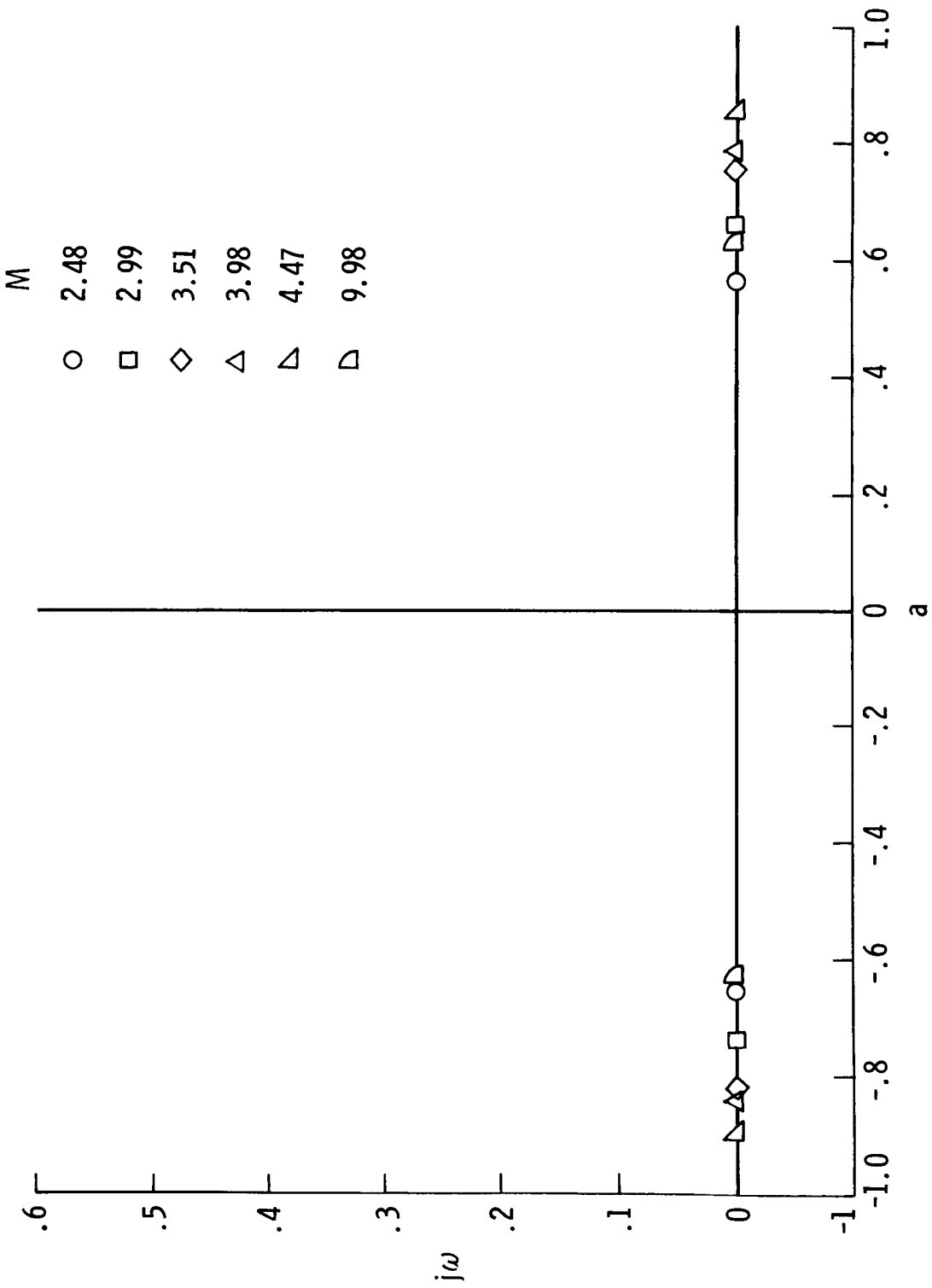
Figure 7.- Roll transfer function (ϕ/δ_a) zeros for normal unaugmented Shuttle configuration.
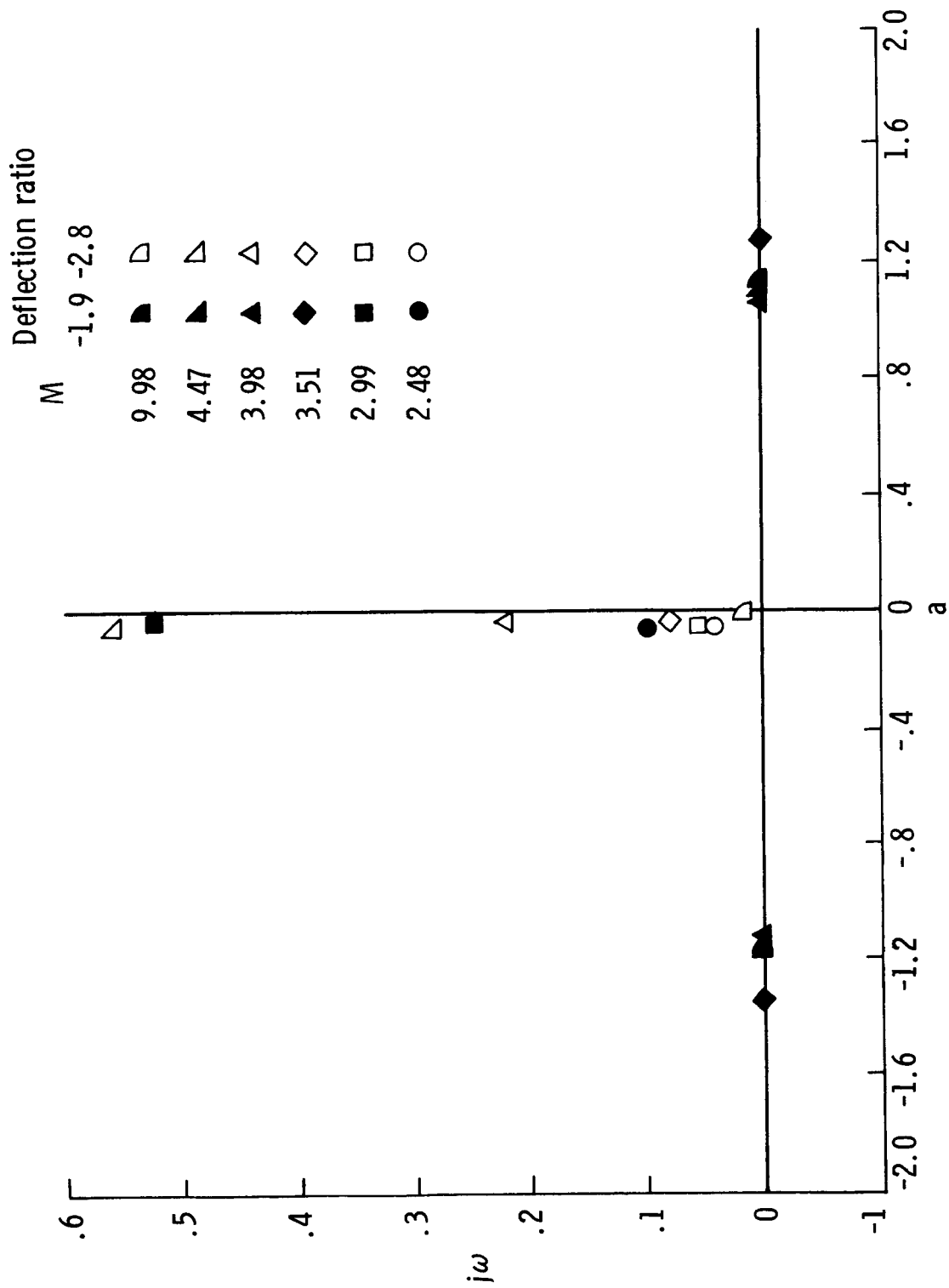
Figure 8.- Roll transfer function (ϕ/δ_c) zeros for deflection ratios of -1.9 and -2.8.
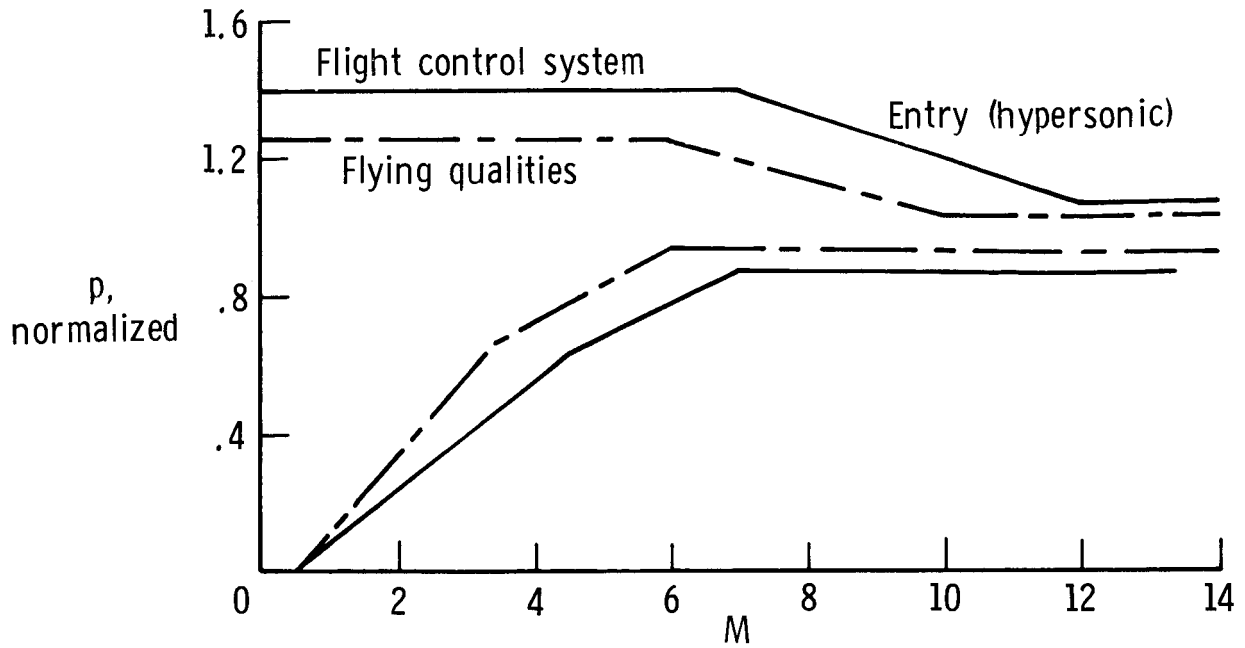
(a) Hypersonic.
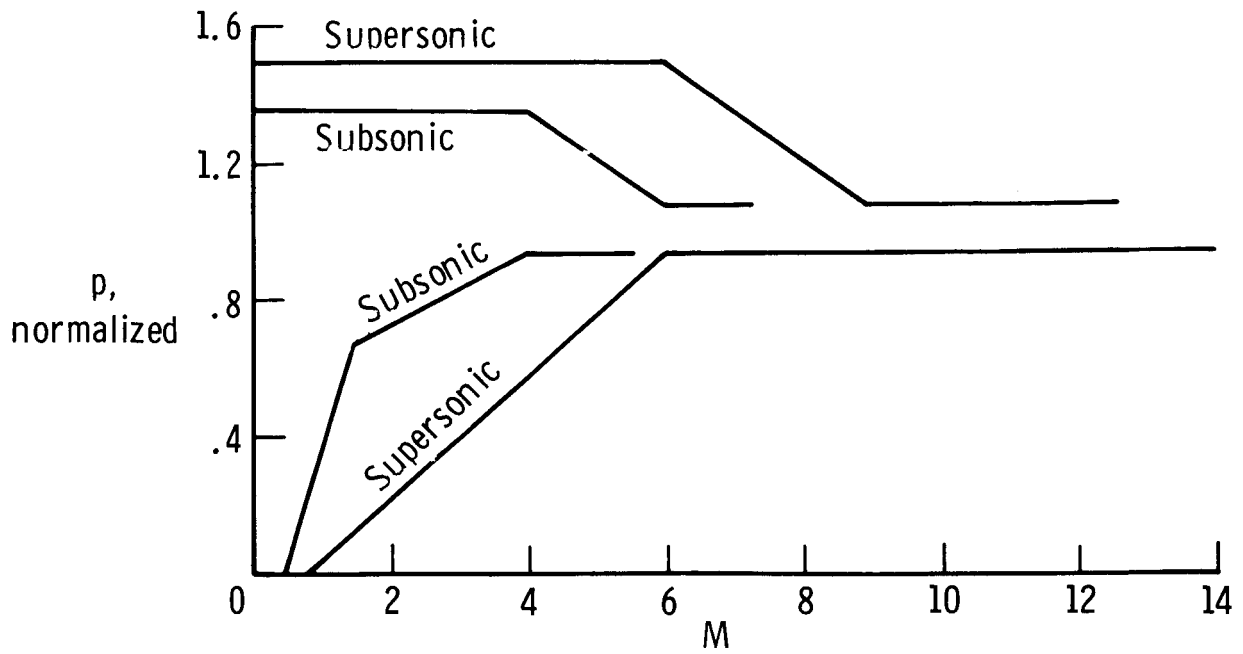
(b) Supersonic and subsonic.

Figure 9.- Normalized roll rate response boundaries.
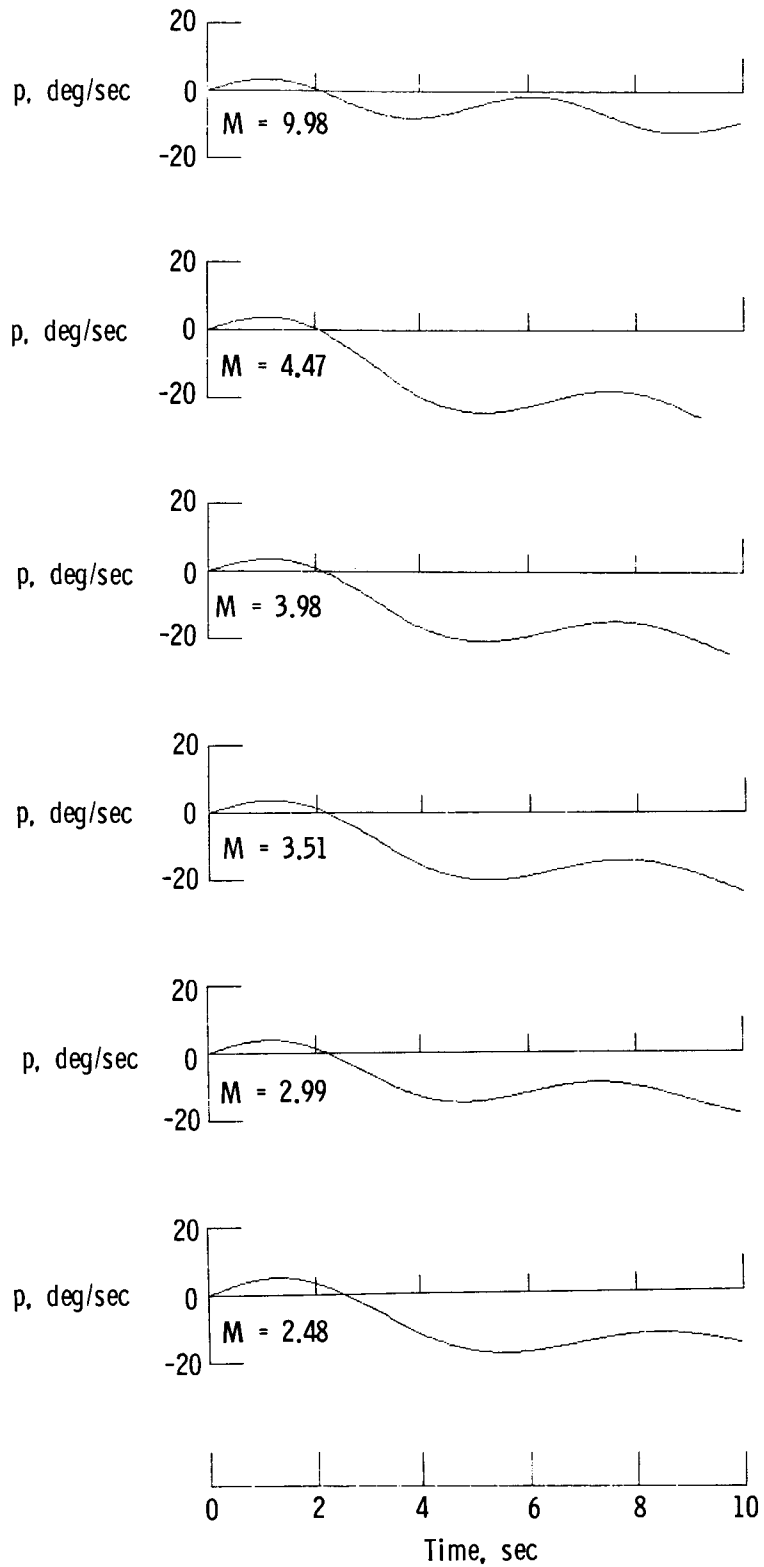
Figure 10.- Lateral responses for normal unaugmented
   Shuttle configuration with aileron step input
   $\delta_a = 2°$.
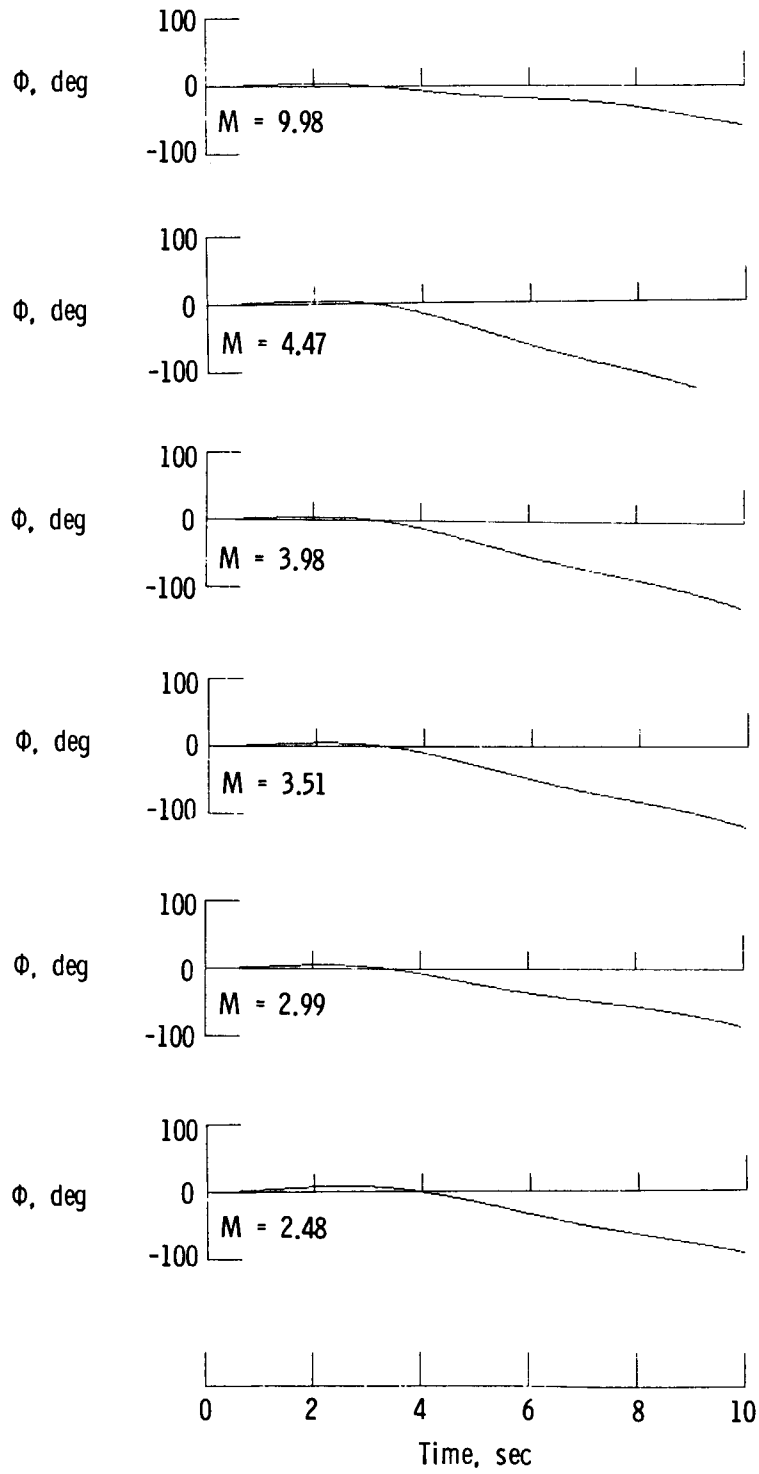
(b) Roll angles.

Figure 10.- Continued.

β, deg

M = 9.98

β, deg

M = 4.47

β, deg

M = 3.98

β, deg

M = 3.51

β, deg

M = 2.99

β, deg

M = 2.48

0   2   4   6   8   10

Time, sec
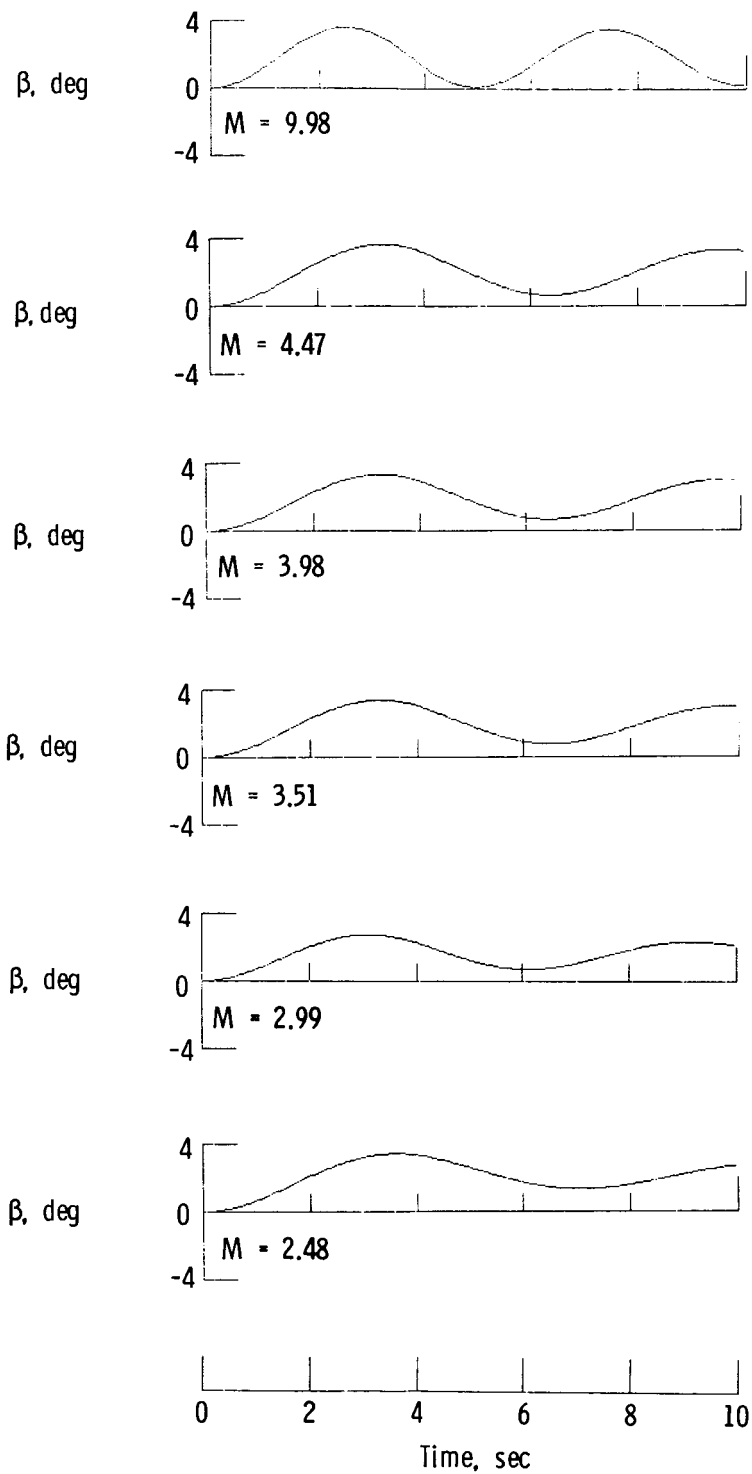
(c) Sideslip angles.

Figure 10.- Concluded.

20

p, deg/ sec 0

M = 9.98

-20

20

p, deg/ sec 0

M = 4.47

-20

20

p, deg/ sec 0

M = 3.98

-20

20

p, deg/ sec 0

M = 3.51

-20

20

p, deg/ sec 0

M = 2.99

-20

20

p, deg/ sec 0

M = 2.48

-20

0   2   4   6   8   10

Time, sec
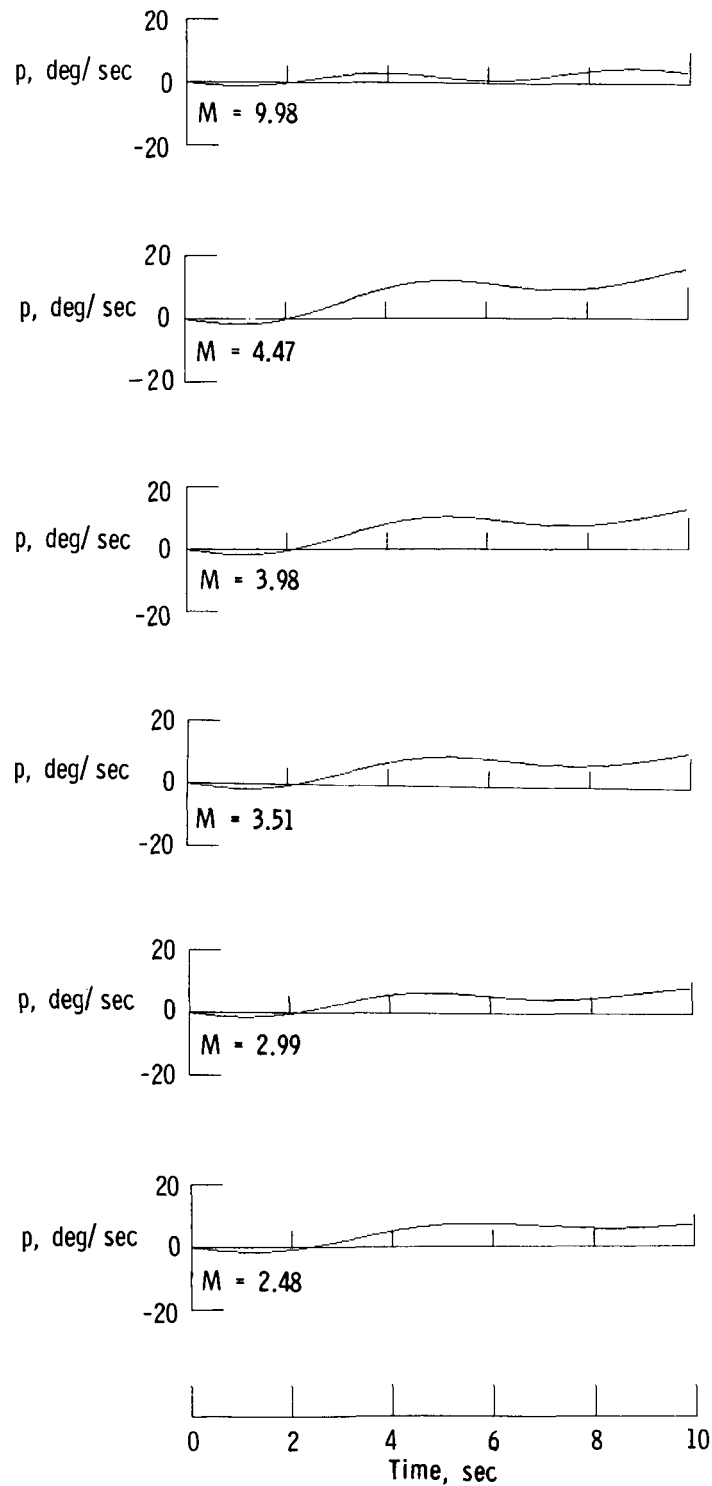
(a) Roll rates.

Figure 11.- Lateral responses for separate-surface configurations with step outboard deflection of $\delta_{OR} = 2°$ for $\delta_{tr,I} = -10°$, $\delta_{tr,O} = 10°$, and $\delta_I/\delta_O = -0$.

Φ, deg

100

0

-100

M = 9.98

Φ, deg

100

0

-100

M = 4.47

Φ, deg

100

0

-100

M = 3.98

Φ, deg

100

0

-100

M = 3.51

Φ, deg

100

0

-100

M = 2.99

Φ, deg

100

0

-100

M = 2.48

0   2   4   6   8   10

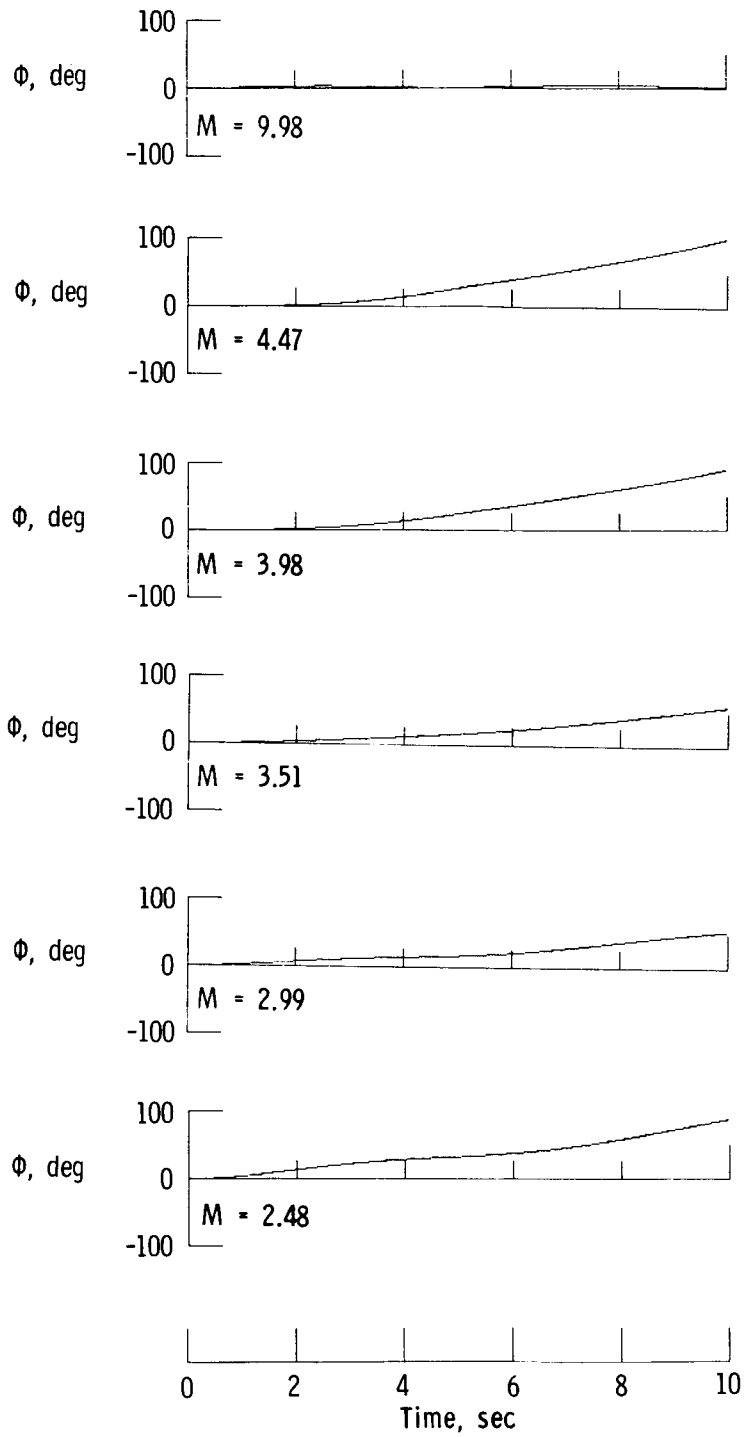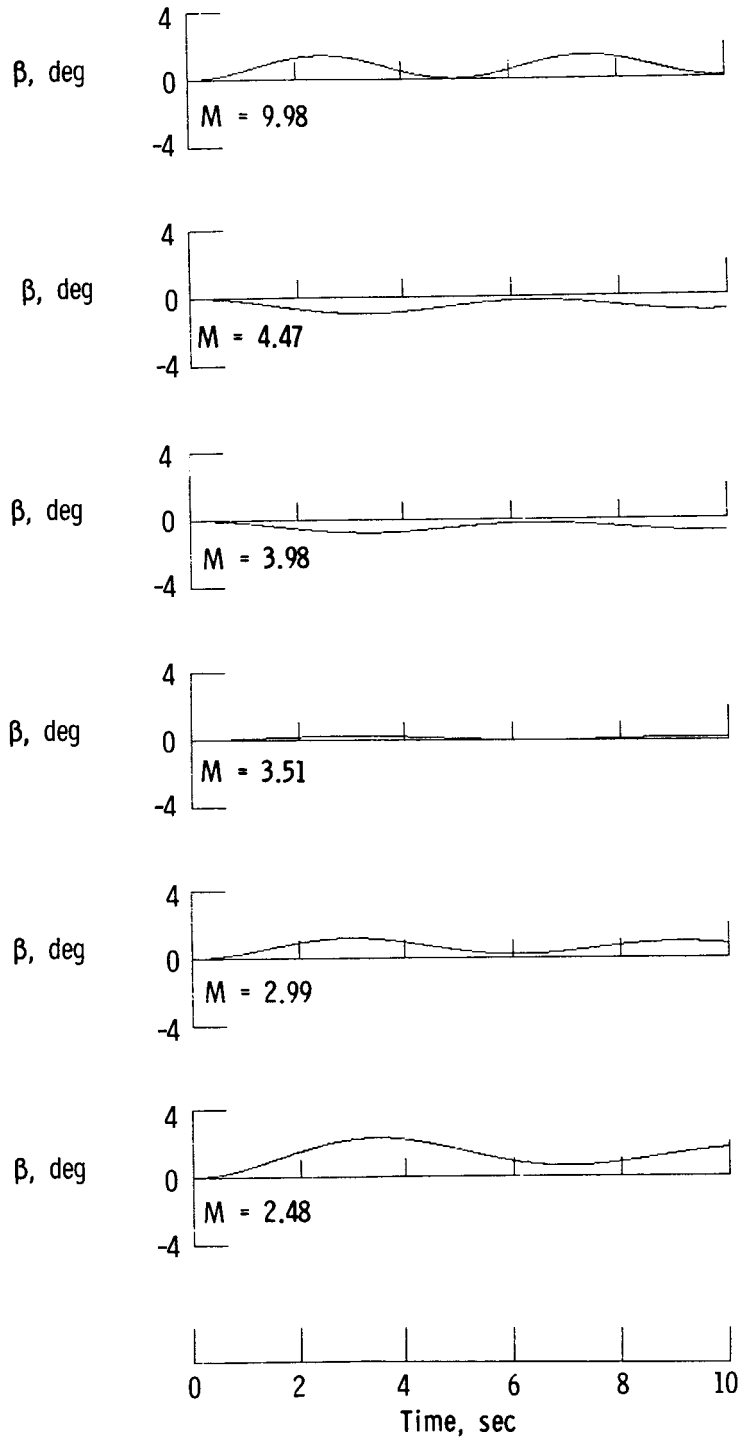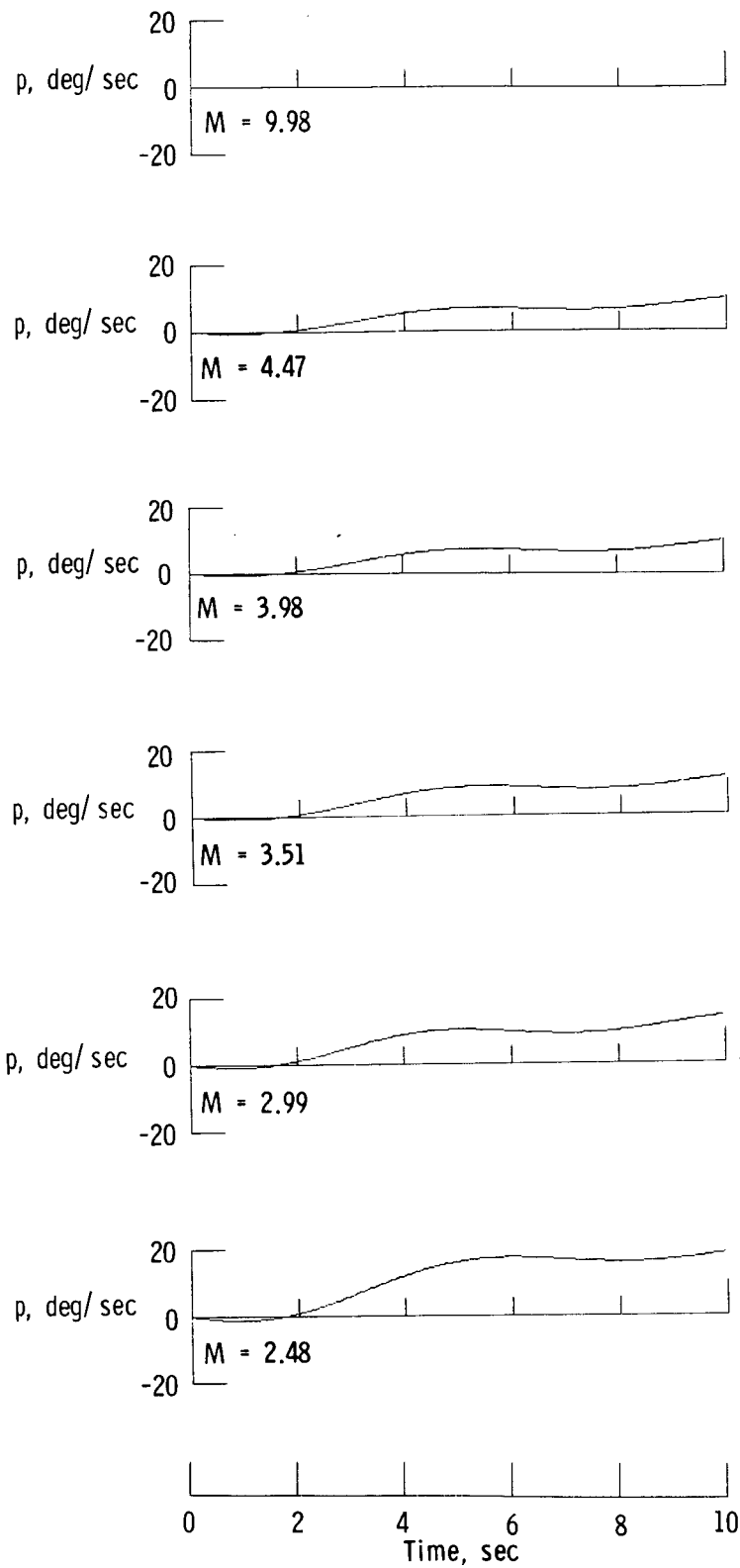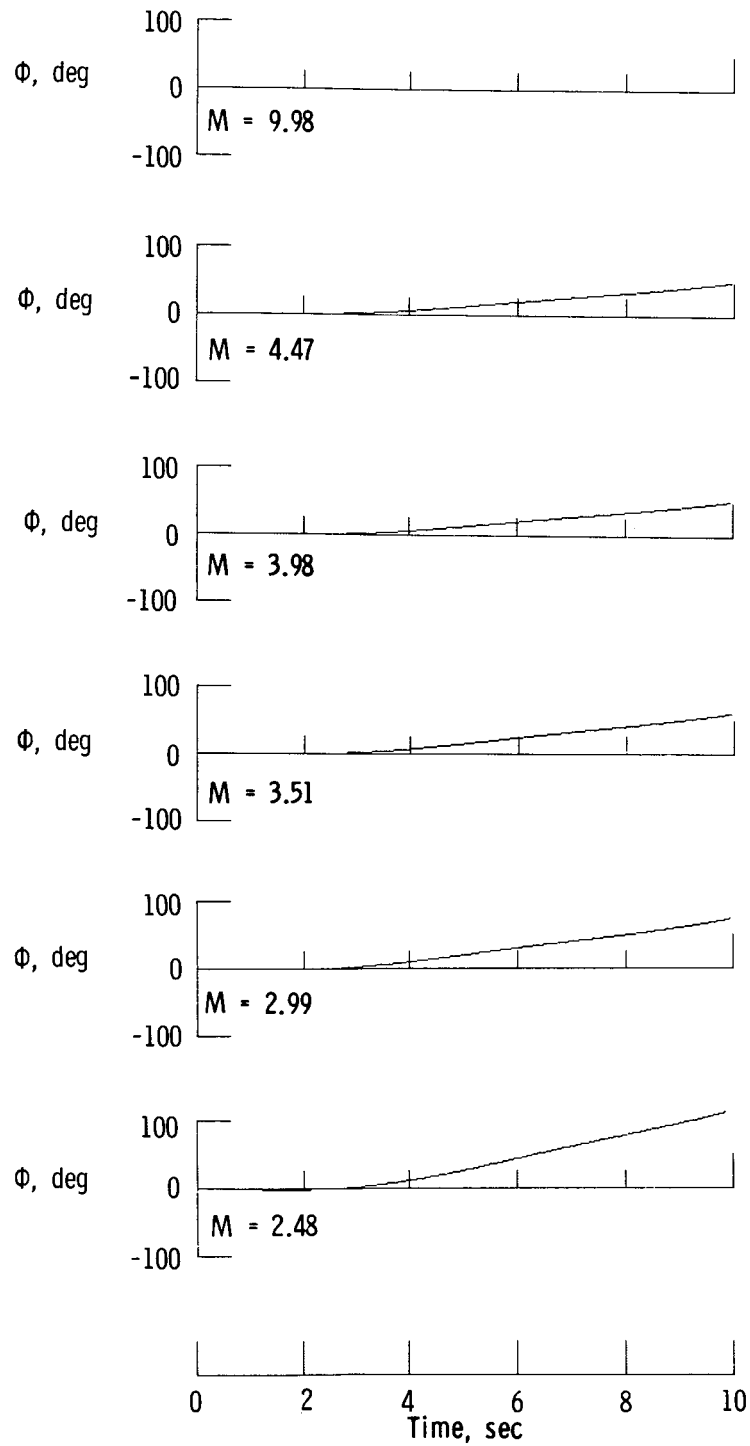Time, sec
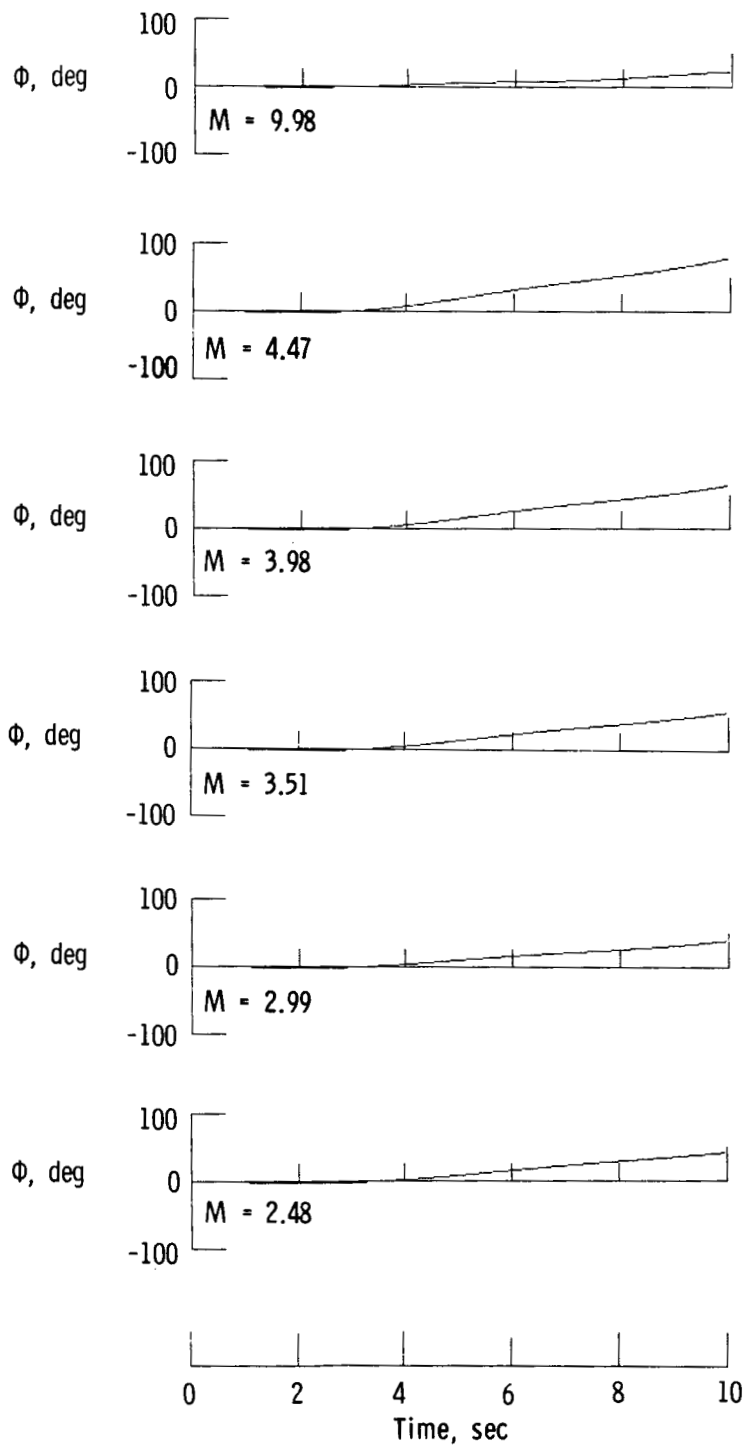
(b) Roll angles.

Figure 11.- Continued.
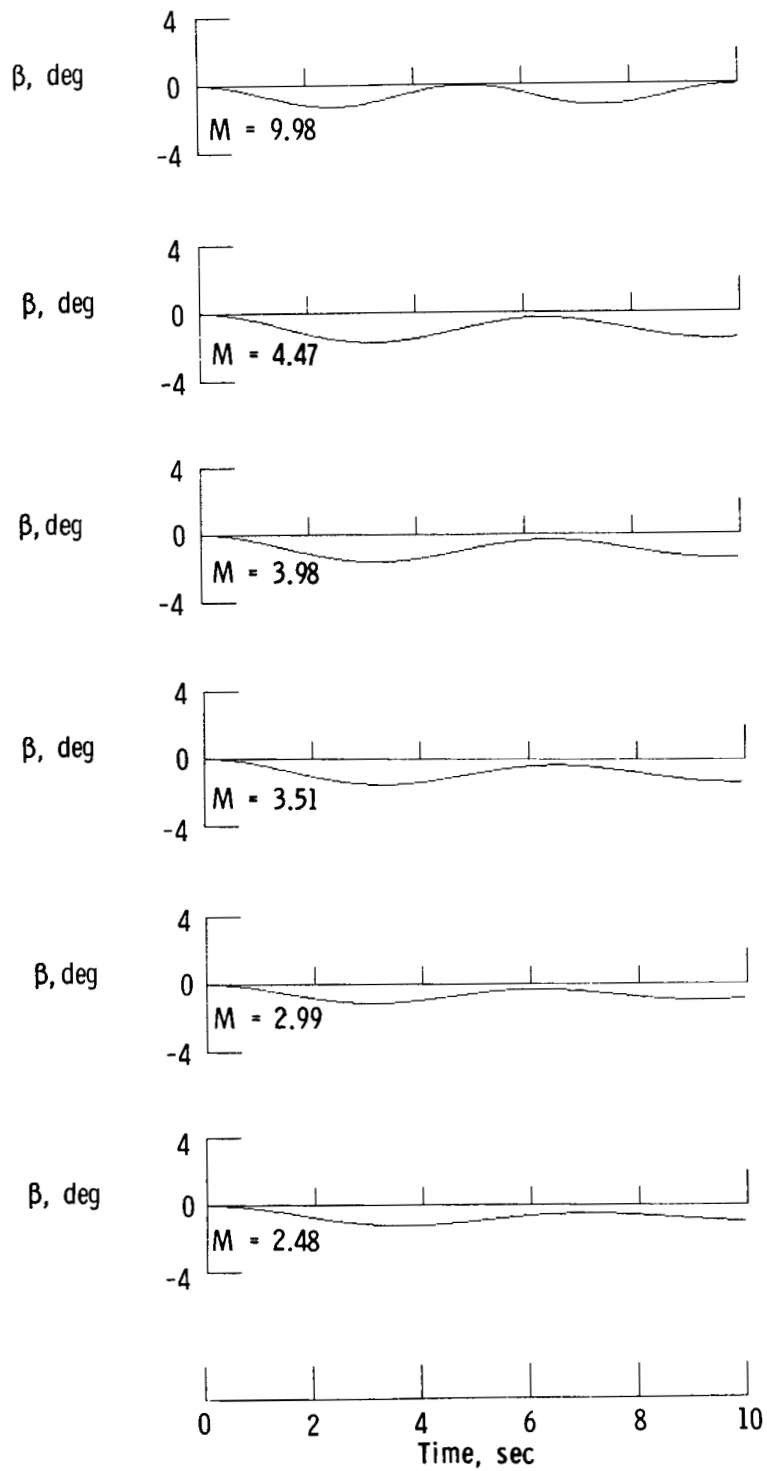
(c) Sideslip angles.

Figure 11.- Concluded.
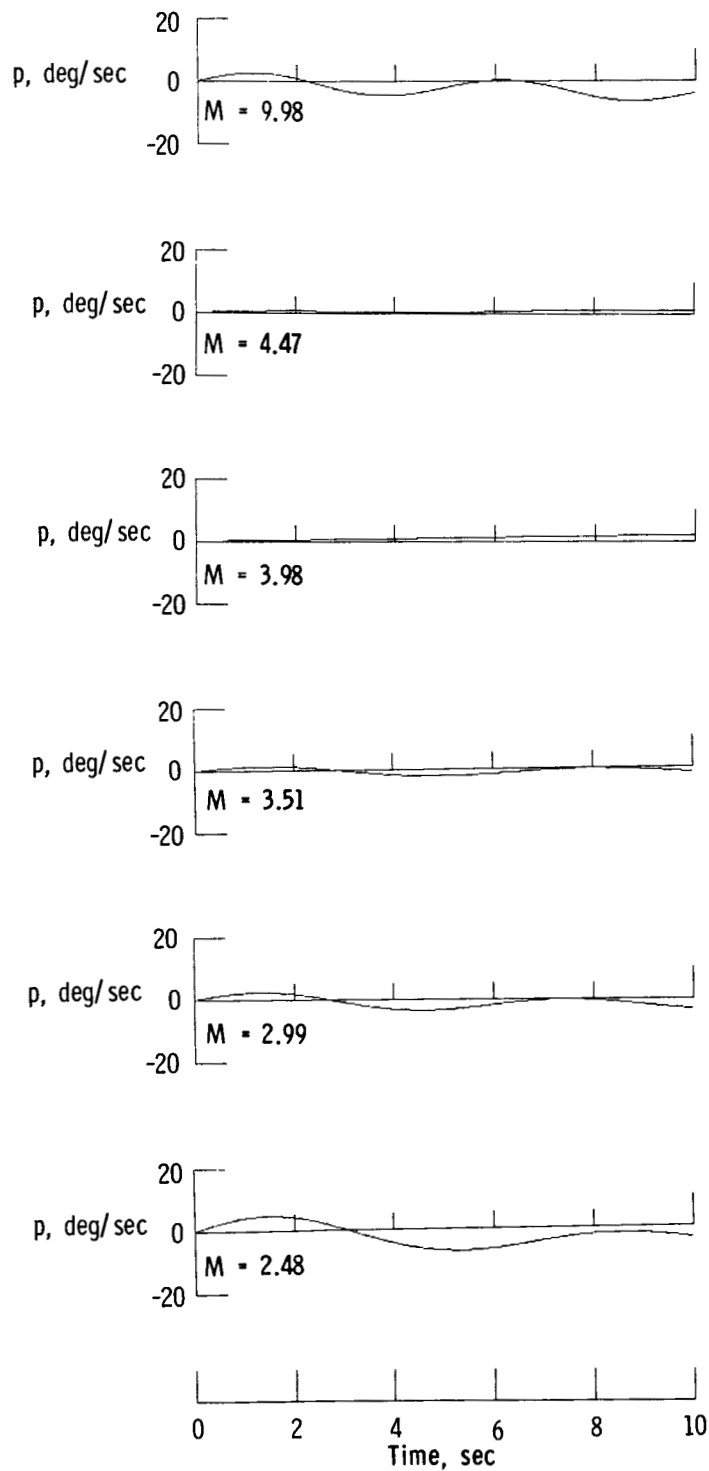
(a) Roll rates.

Figure 12.- Lateral responses for separate-surface
configuration with step control input of $\delta_c = 10°$
for $\delta_{tr,I} = 0°$, $\delta_{tr,O} = 10°$, and $\delta_I/\delta_O = -1.9$.
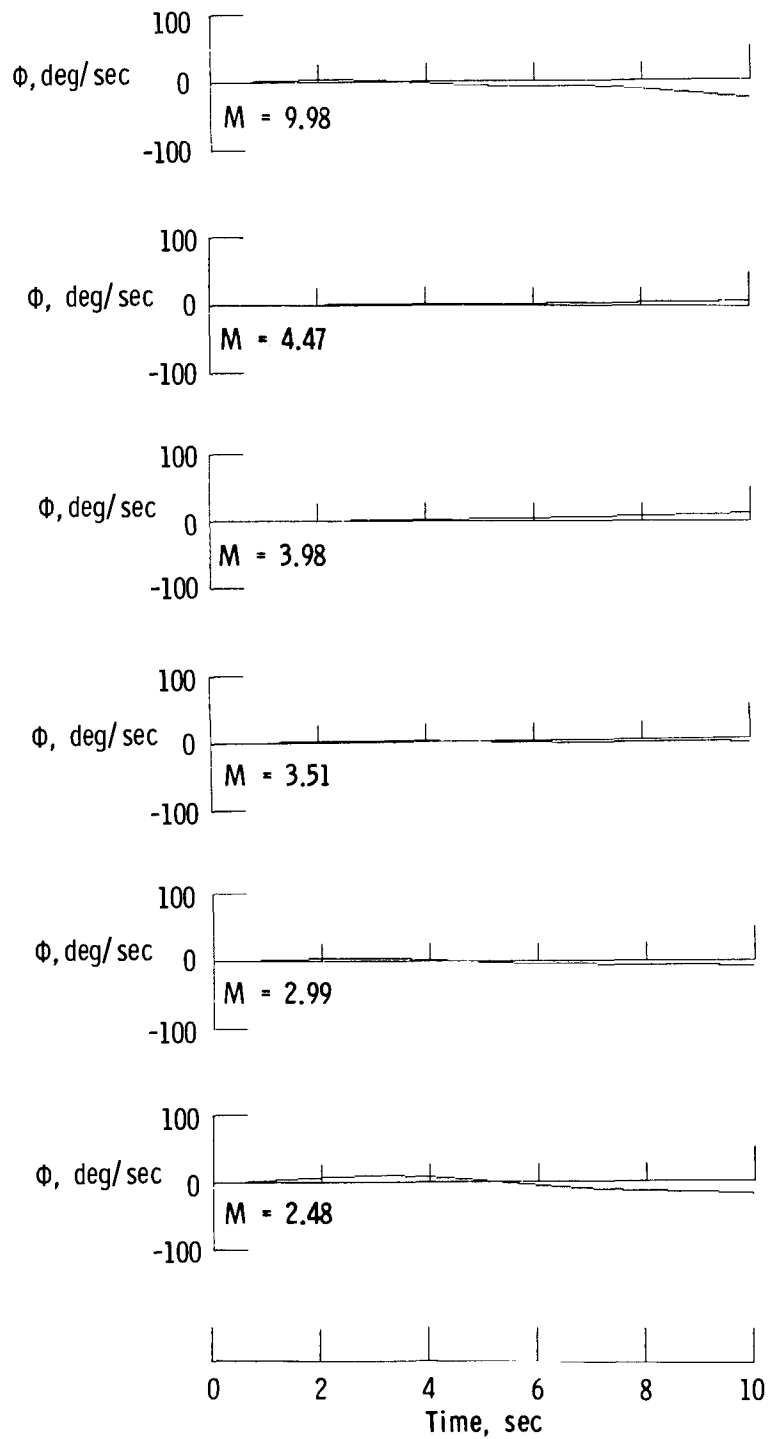
(b) Roll angles.

Figure 12.- Continued.
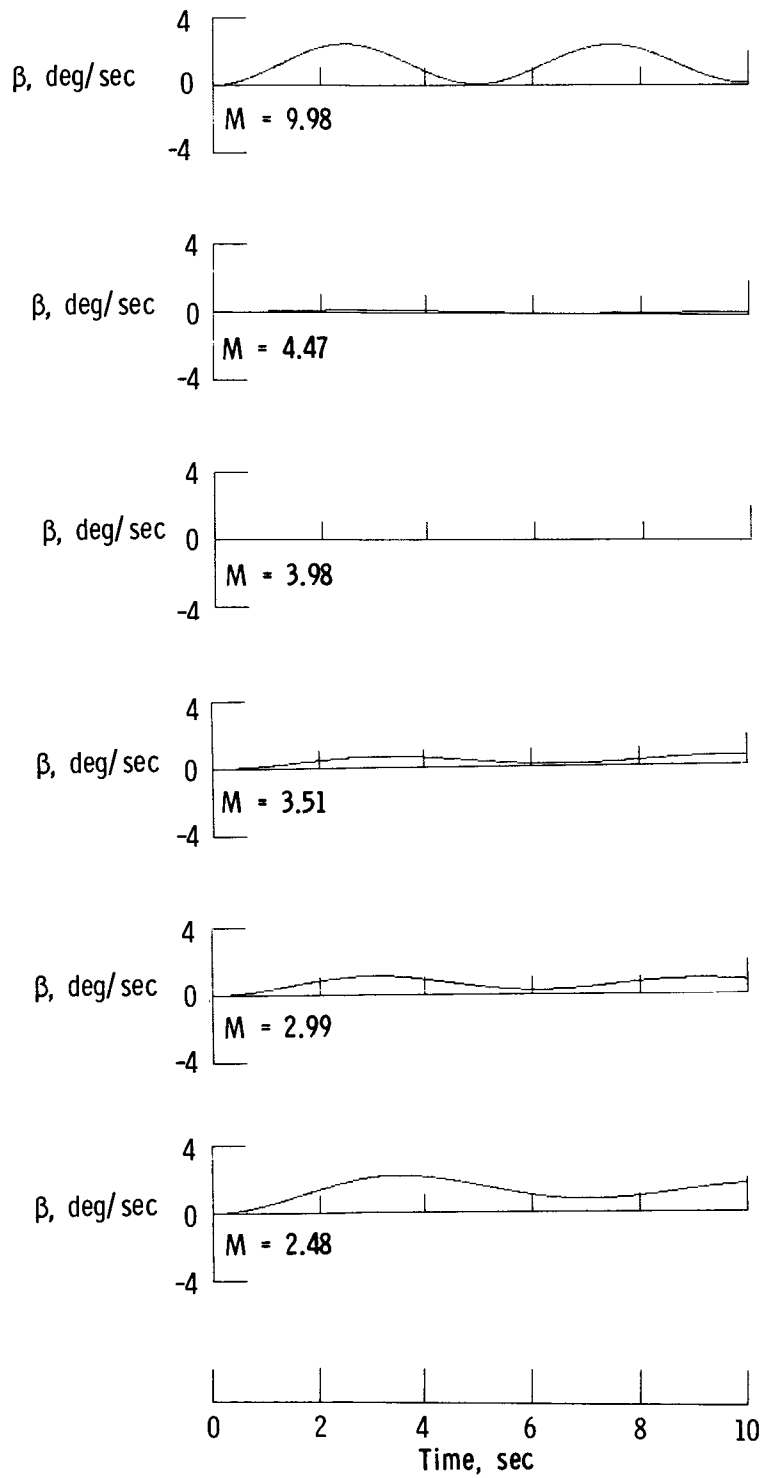
(c) Sideslip angles.

Figure 12.- Concluded.

20

p, deg/sec   0

M = 9.98

-20

20

p, deg/sec   0

M = 4.47

-20

20

p, deg/sec   0

M = 3.98

-20

20

p , deg/sec   0

M = 3.51

-20

20

p, deg/sec   0

M = 2.99

-20

20

p, deg/sec   0

M = 2.48

-20

0   2   4   6   8   10
Time, sec
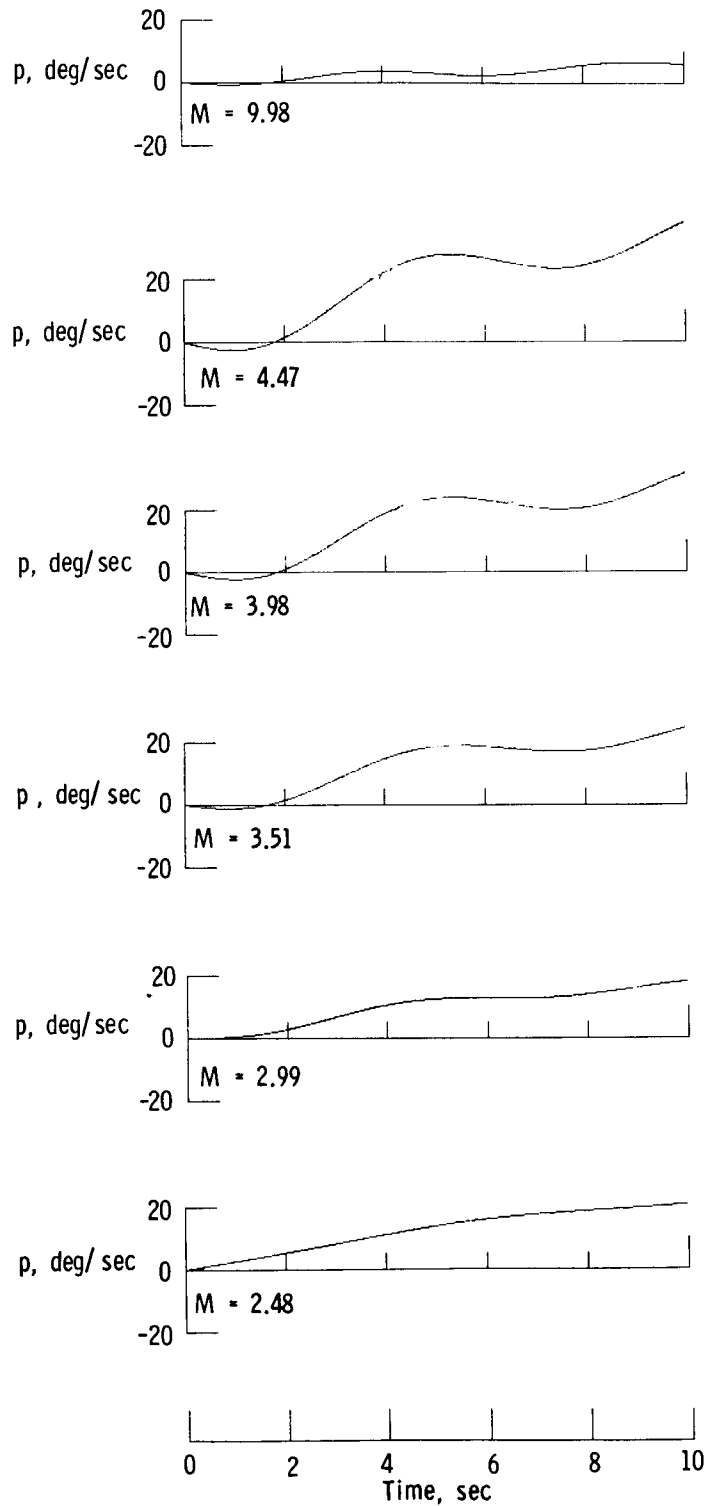
(a) Roll rates.

Figure 13.- Lateral responses for separate-surface
configuration with step control input of $\delta_c = 10°$
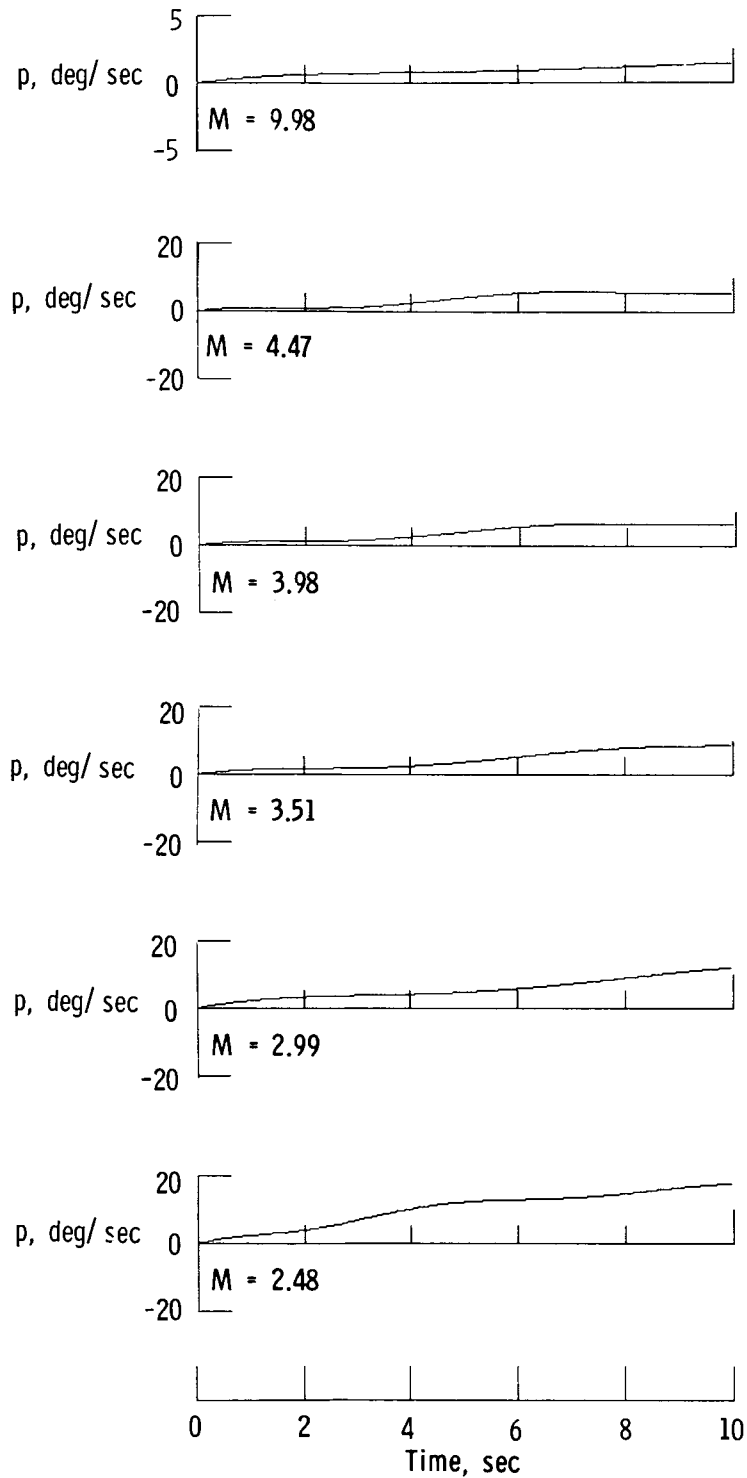for $\delta_{tr,I} = -10°$, $\delta_{tr,O} = 10°$, and $\delta_I/\delta_O = -1.9$.
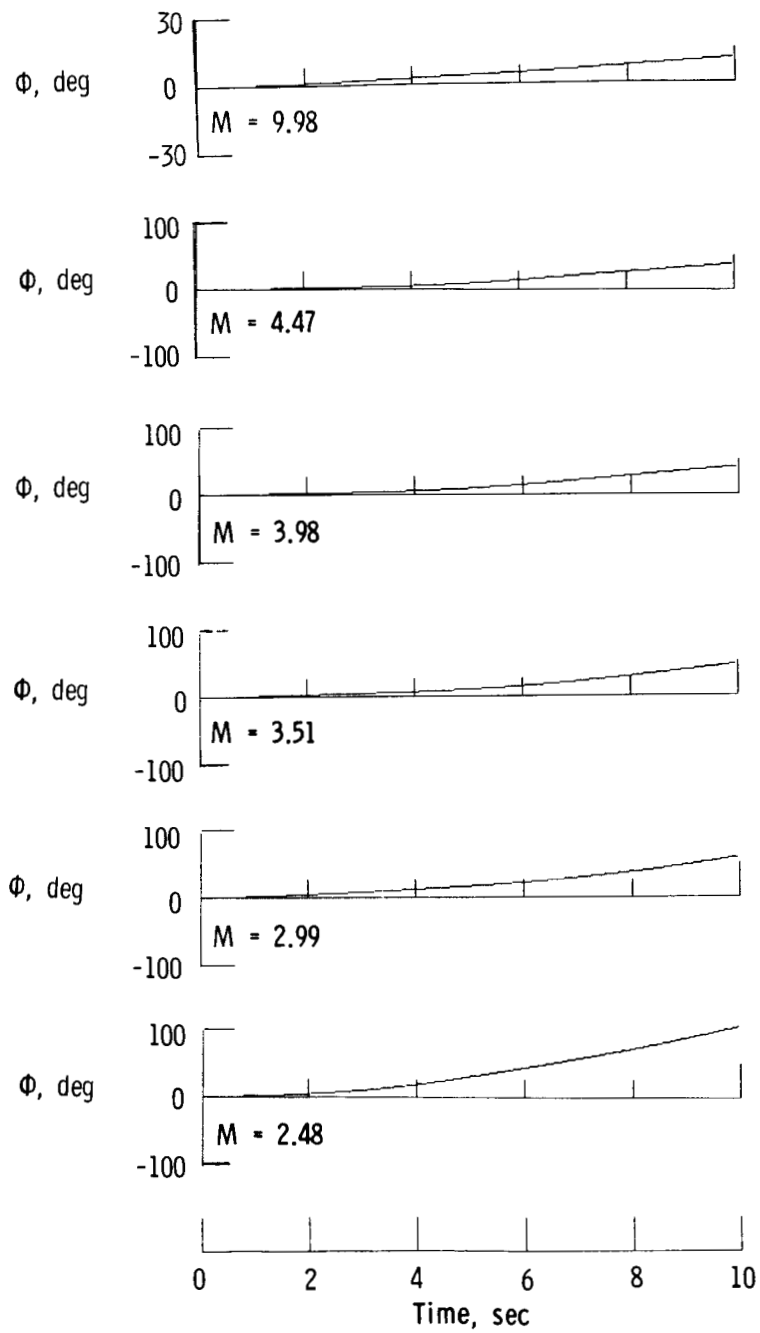
42
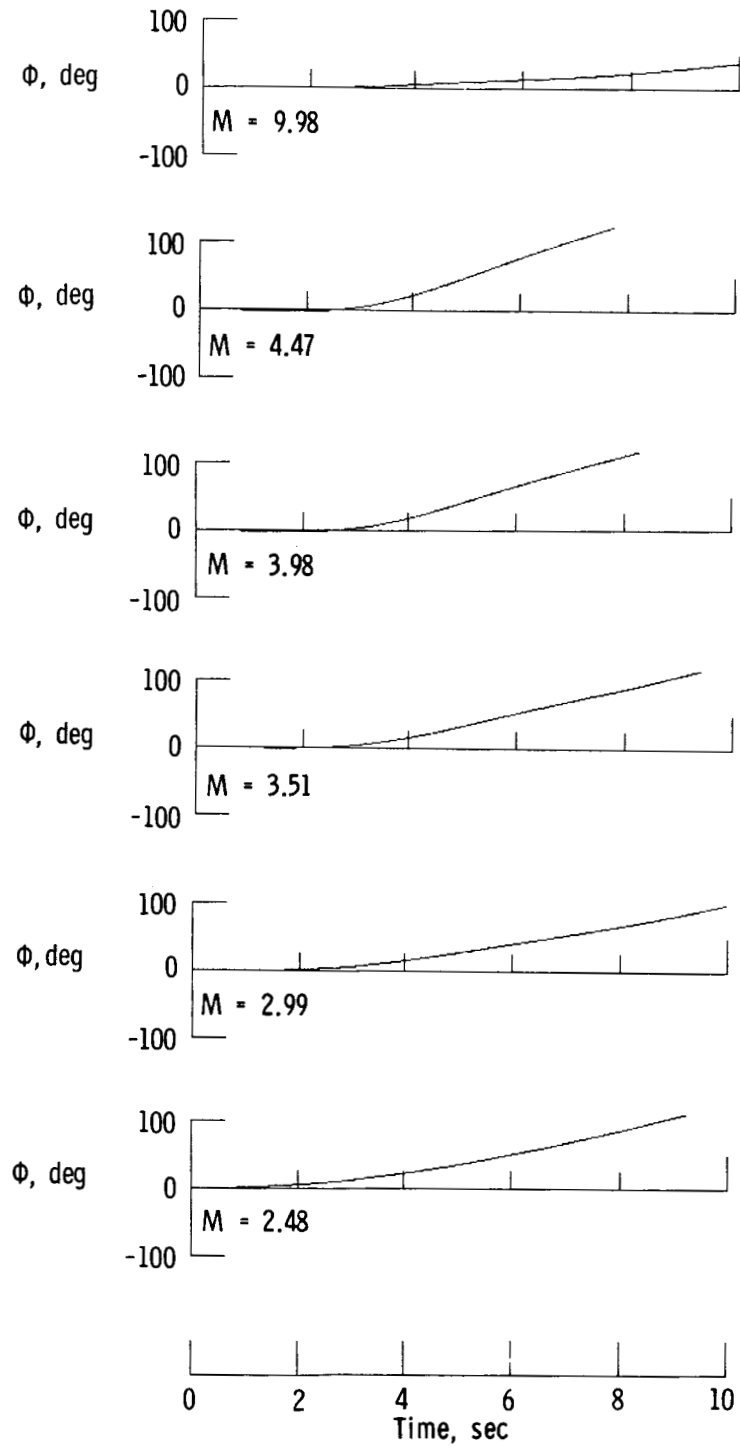
(b) Roll angles.

Figure 13.- Continued.
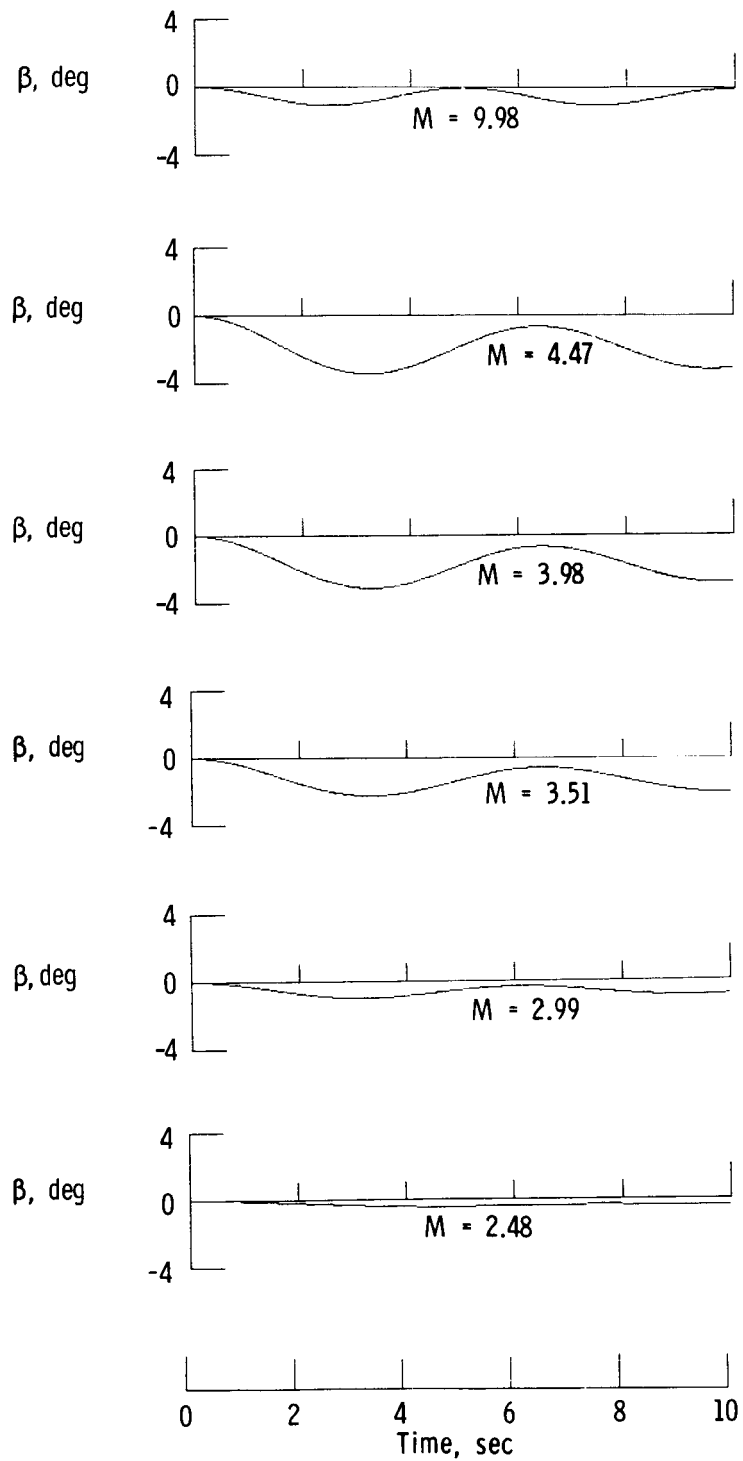
(c) Sideslip angles.

Figure 13.- Concluded.
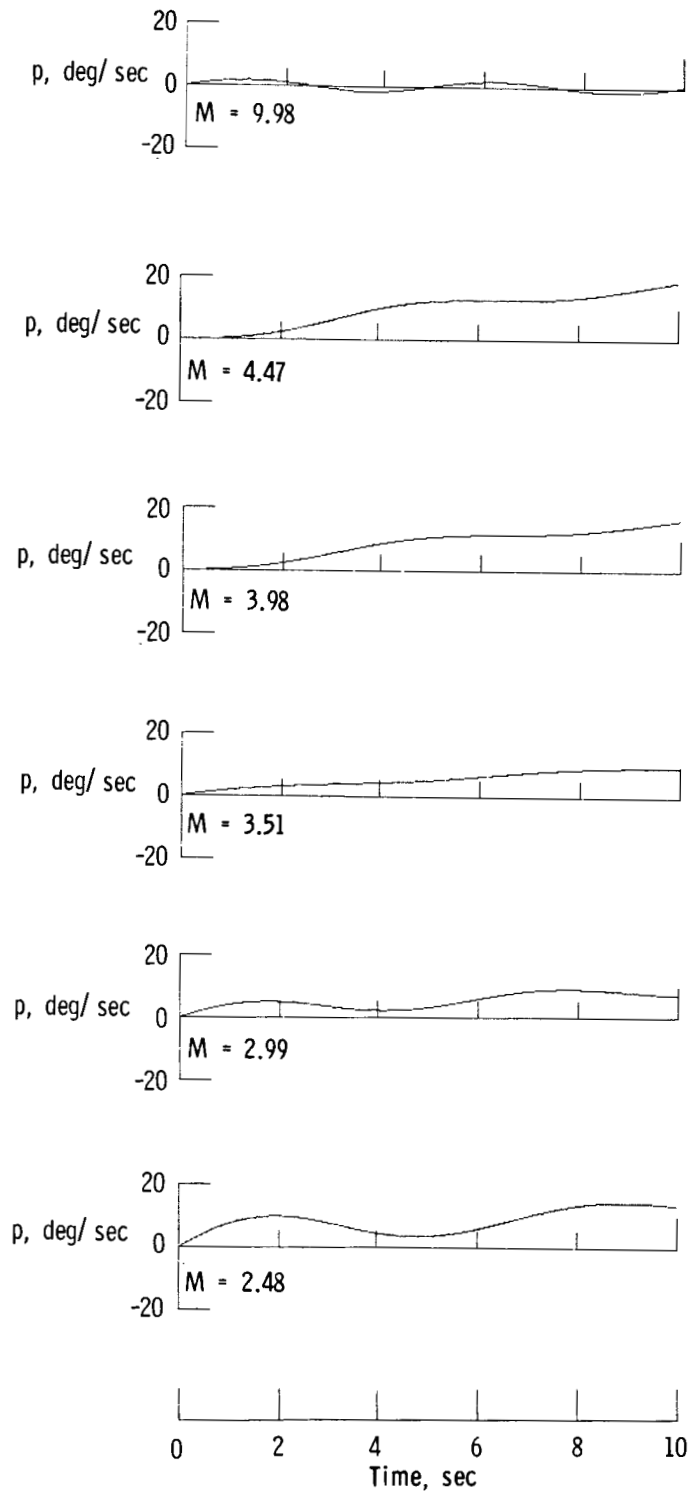
(a) Roll rates.

Figure 14.- Lateral responses for separate-surface
   configuration with step control input of
   $\delta_c = 10°$ for $\delta_{tr,I} = -10°$, $\delta_{tr,O} = 10°$,
   and $\delta_I/\delta_O = -2.8$.

(b) Roll angles.

Figure 14.- Continued.

(c) Sideslip angles.

Figure 14.- Concluded.

(a) Roll rates.

Figure 15.- Lateral responses for separate-surface configuration with rudder input of $\delta_r = -2°$ for $\delta_{tr,I} = -10°$, and $\delta_{tr,O} = 10°$.

(b) Roll angles.

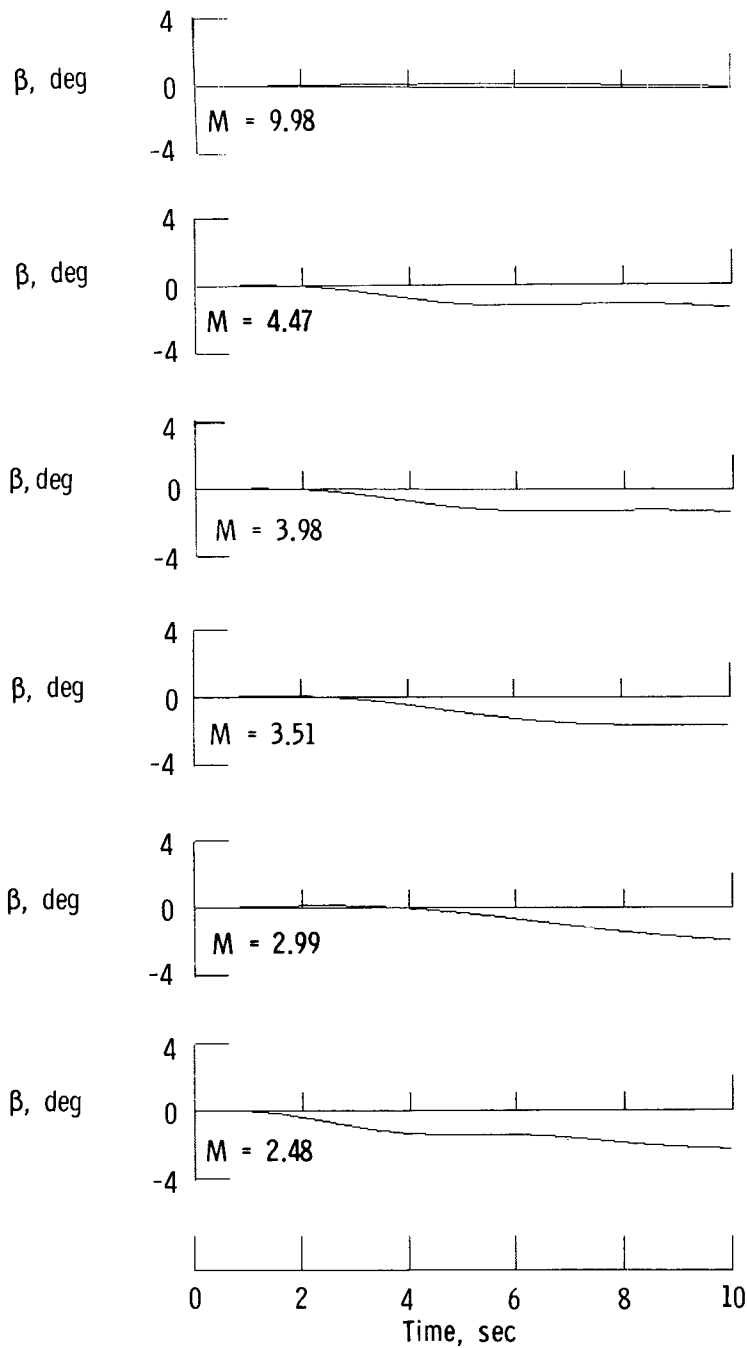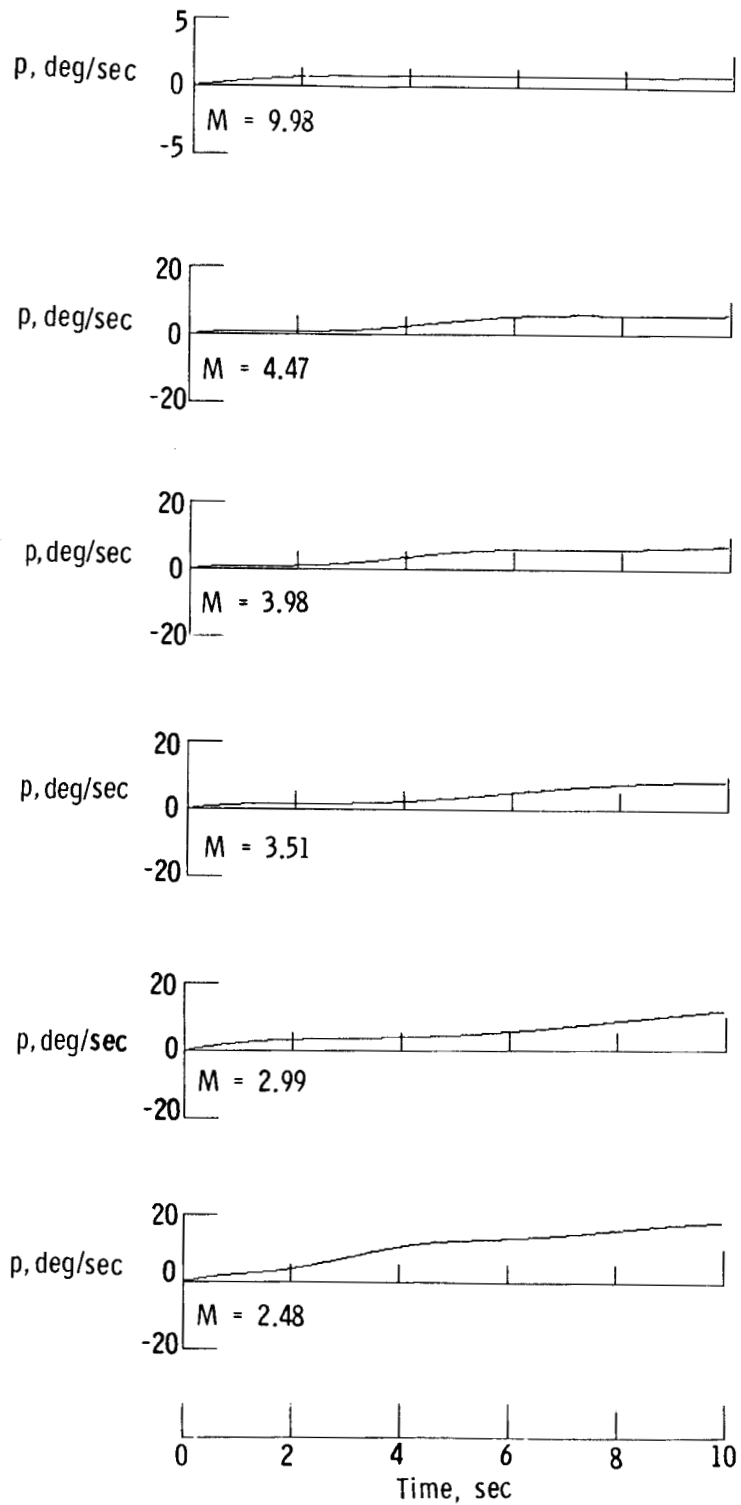Figure 15.- Continued.
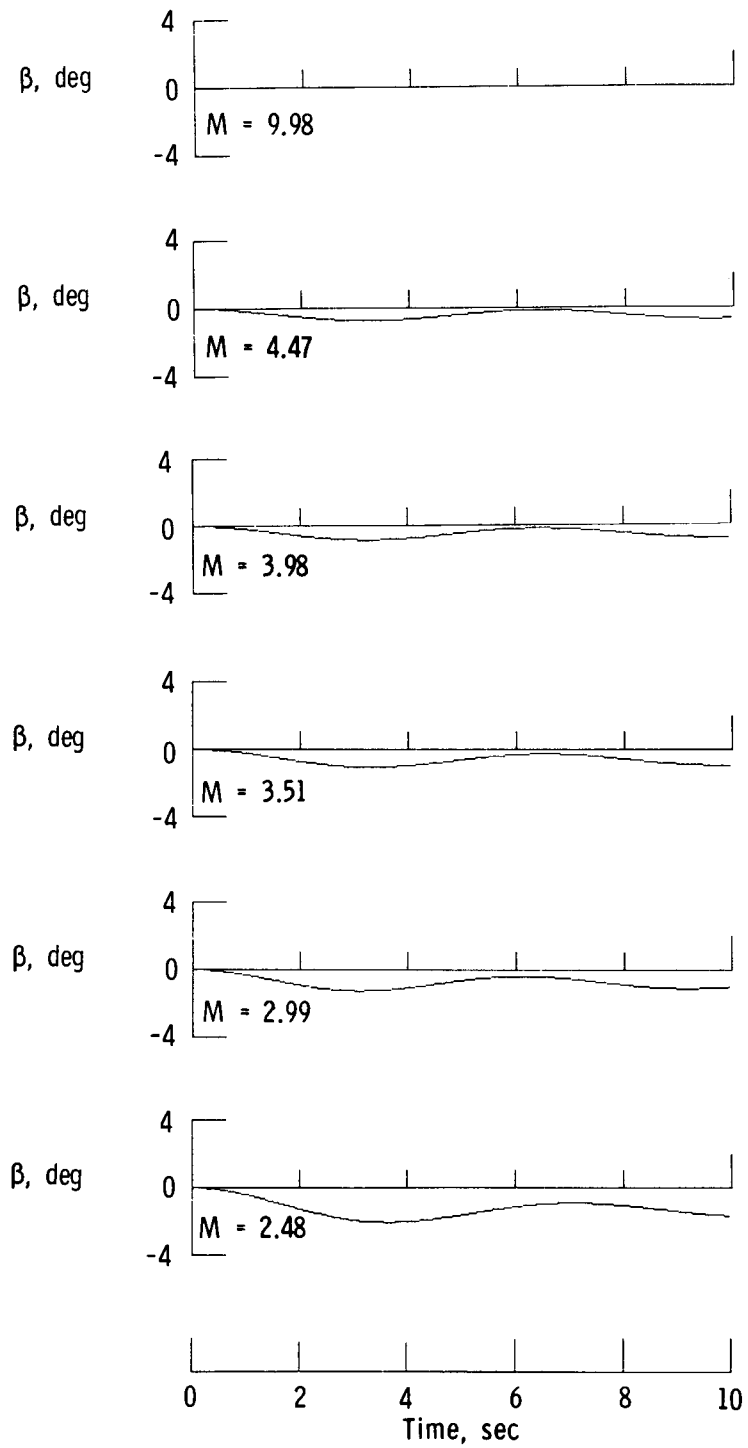
(c) Sideslip angles.

Figure 15.- Concluded.

(a) Roll rates.

Figure 16.- Lateral responses for augmented separate-surface configuration for $\delta_c = 10°$, $\delta_{tr,I} = -10°$, $\delta_{tr,O} = 10°$, and $\delta_I/\delta_O = -2.8$.

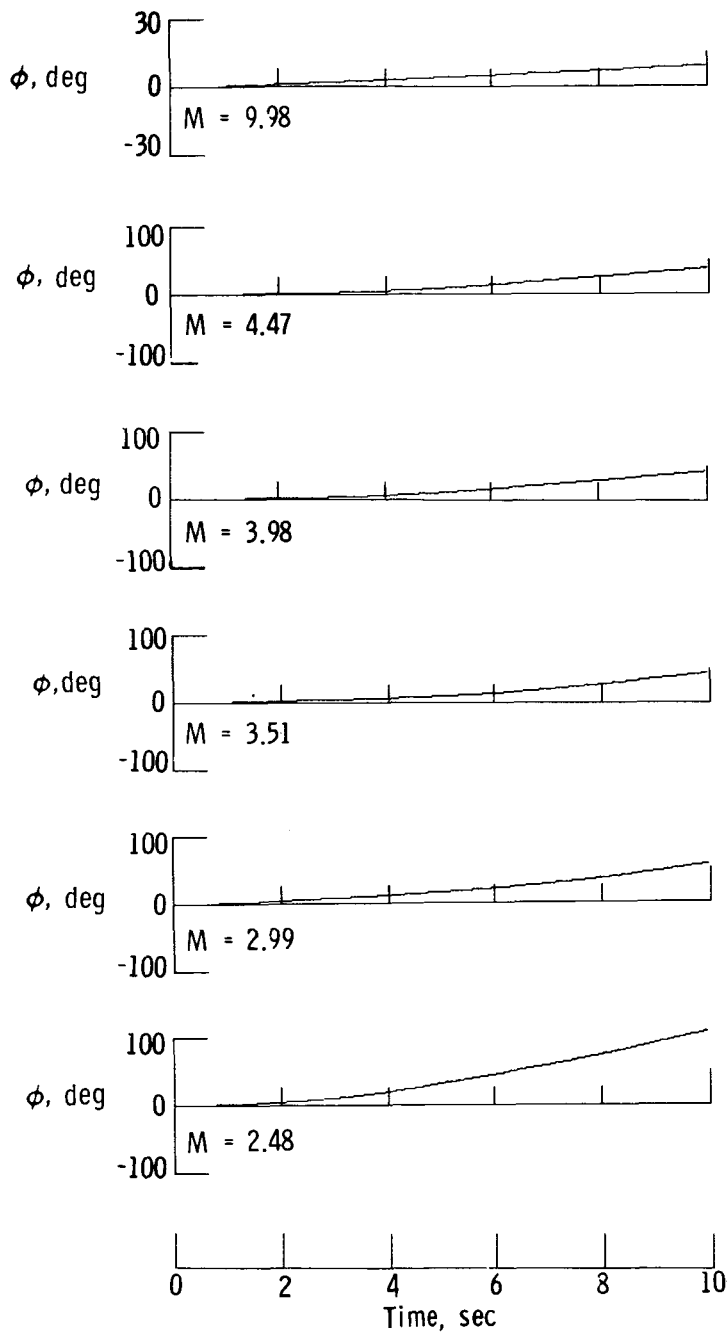(b) Roll angles.

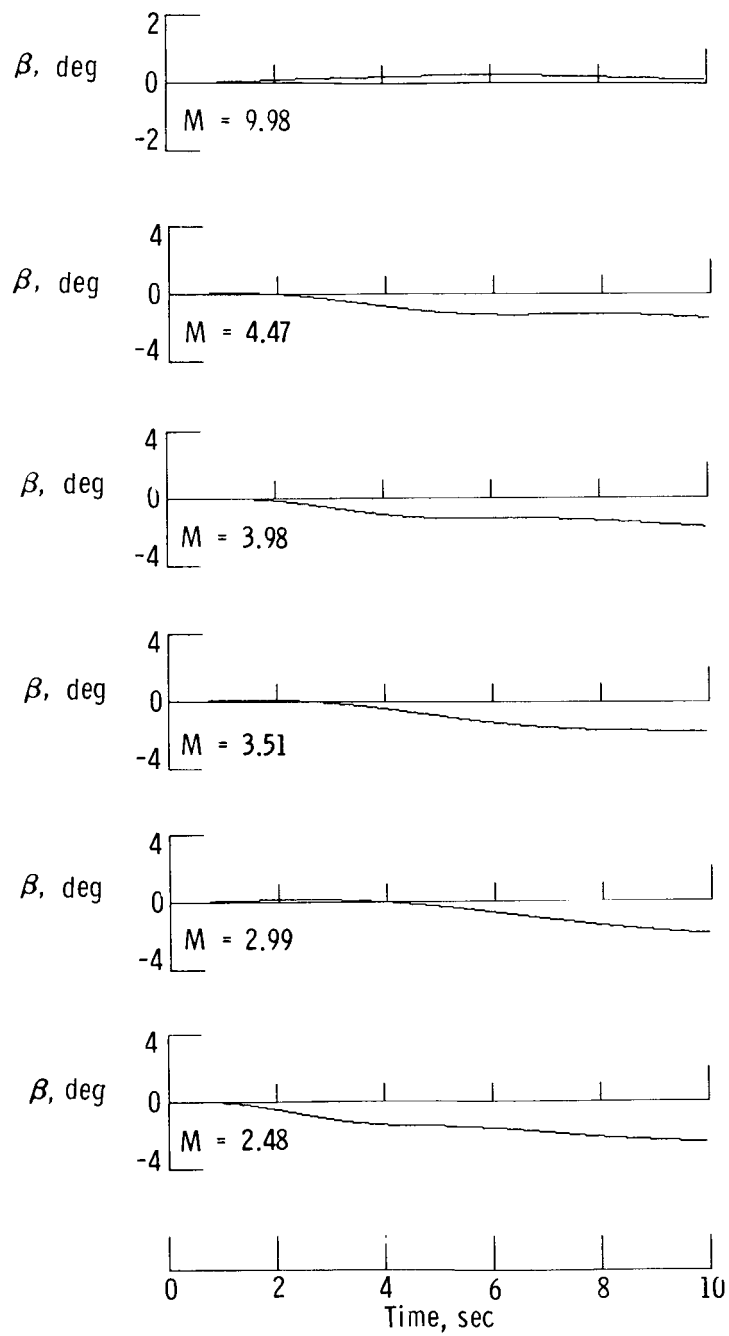Figure 16.- Continued.

(c) Sideslip angles.

Figure 16.- Concluded.

(a) Roll rates.

Figure 17.- Lateral responses for augmented separate-surface configuration to indicate sensitivity with $\delta_c = 10°$, $\delta_{tr,I} = -10°$, $\delta_{tr,O} = 10°$, and $\delta_I/\delta_O = -2.8.$

(b) Roll angles.

Figure 17.- Continued.

(c) Sideslip angles.

Figure 17.- Concluded.

1. Report No. NASA TP-2340	2. Government Accession No.	3. Recipient's Catalog No.

4. Title and Subtitle	5. Report Date
SPACE SHUTTLE SEPARATE-SURFACE CONTROL-SYSTEM STUDY	July 1984
	6. Performing Organization Code 505-34-03-02

7. Author(s) Lawrence W. Brown and Raymond C. Montgomery	8. Performing Organization Report No. L-15650
9. Performing Organization Name and Address	10. Work Unit No.
NASA Langley Research Center Hampton, VA 23665	11. Contract or Grant No.
12. Sponsoring Agency Name and Address	13. Type of Report and Period Covered Technical Paper
National Aeronautics and Space Administration Washington, DC 20546	14. Sponsoring Agency Code

15. Supplementary Notes

16. Abstract

A control-system concept is presented that produces proportional control of yaw moment for the Space Shuttle from early entry to Mach 2 with only software modifications of the vehicle. It uses separate deflections of the inboard and outboard elevon surfaces and is evaluated, first, by determining the maximum static yawing moment available by considering the deflection limits of the elevon surfaces. Results indicate that a proportional moment slightly in excess of that produced by the most effective reaction control system (RCS) jet for yaw control can be obtained. In addition to the static-moment study, a control law was designed which was intended to produce desired flying qualities. These flying qualities were taken from the military specifications for class III piloted transport aircraft and may not be appropriate for the Space Shuttle in early entry. For Mach numbers less than 5, the design goal was realized; however, near Mach 10, it was not. The failure to achieve the specified design goal may be the result of inappropriately selected goals.

17. Key Words (Suggested by Author(s))	18. Distribution Statement
Space Shuttle Proportional control Aerodynamic characteristics Separated surfaces Inboard and outboard elevon surfaces	Unclassified – Unlimited Subject Category 08

19. Security Classif. (of this report) Unclassified	20. Security Classif. (of this page) Unclassified	21. No. of Pages 57	22. Price A04